

JAERI-M  
84-160

STUDIES ON CRYOGENIC DISTILLATION  
COLUMNS FOR HYDROGEN ISOTOPE  
SEPARATION

August 1984

Masahiro KINOSHITA

日本原子力研究所  
Japan Atomic Energy Research Institute

JAERI-M レポートは、日本原子力研究所が不定期に公刊している研究報告書です。

入手の間合わせは、日本原子力研究所技術情報部情報資料課（〒319-11 茨城県那珂郡東海村）あて、お申しこしてください。なお、このほかに財団法人原子力弘済会資料センター（〒319-11 茨城県那珂郡東海村日本原子力研究所内）で複写による実費頒布をおこなっております。

JAERI-M reports are issued irregularly.

Inquiries about availability of the reports should be addressed to Information Section, Division of Technical Information, Japan Atomic Energy Research Institute, Tokai-mura, Naka-gun, Ibaraki-ken 319-11, Japan.

© Japan Atomic Energy Research Institute, 1984

---

編集兼発行 日本原子力研究所  
印 刷 山 田 軽 印 刷 所

STUDIES ON CRYOGENIC DISTILLATION COLUMNS FOR HYDROGEN ISOTOPE  
SEPARATION

Masahiro KINOSHITA

Department of Thermonuclear Fusion Research

Tokai Research Establishment, JAERI

( Received August 10, 1984 )

Cryogenic distillation is applicable to a number of situations. The feed condition, column cascade configuration, input and output specifications vary greatly from situation to situation. In the mainstream fuel circulation system for a fusion reactor, the feed composition may fluctuate greatly during the operation. The radiological standards for tritium lost to the environment are increasingly becoming stricter. Systematic studies are needed to achieve the goal of long-term operation meeting the strict requirements for products even under great fluctuation of the feed condition in all the situations.

The present report gives a critical, brief review of the studies which have been made by the author. The subjects treated are development of computer simulation procedures, analysis on an H-T separation column with a feedback stream, dynamics and control, proposal of a new cascade, analysis on helium effects on column behavior, start-up analysis for a cascade, and preliminary experimental study on dependence of HETP on operational conditions.

KEYWORDS : Cryogenic Distillation, Isotope Separation, Hydrogen Isotopes, Fusion Reactor, Tritium System, Column Cascade, Feedback Stream, Dynamics, Control, Start-Up, HETP

水素同位体分離のための深冷蒸留塔に関する研究

日本原子力研究所東海研究所核融合研究部

木下正弘

(1984年8月10日受理)

深冷蒸留法は、多くの場合に適用できる。フィードの条件、塔カスケード構成、入出力条件は、各場合によって大きく異なる。核融合炉の燃料給排気システムにおいては、フィードの組成は操作中にかなり変動する可能性がある。環境へのトリチウム放出量に対する規制は、ますます厳しくなりつつある。すべての場合において、フィードの条件が大きく変動しても、厳しい出力条件を満たした長期的な操作が行えるようにするという目標を達成するためには、系統的な研究が不可欠となる。

本報は、著者の現在までの研究を批評的にレビューしたものである。対象となるテーマは、シミュレーション手法の開発、フィードバック流れを持つH-T分離塔の特性、動特性及び制御に関する解析、1つの新しいカスケードの提案、ヘリウムが塔特性に及ぼす影響、塔カスケードのスタートアップに関する解析、及びHETPの操作条件への依存性に関する実験的研究である。

## CONTENTS

1.	INTRODUCTION	...	1
1.1	Scope and significance of the present report.	...	1
1.2	Outline of the present report.	...	4
	REFERENCES	...	5
	Figures	...	6
2.	STEADY STATE SIMULATION	...	8
2.1	A simulation procedure for hydrogen isotope distillation columns in tritium systems.	...	8
2.2	Determination procedures for initial values of the independent variables.	...	9
2.3	Effects of decay heat of tritium and nonideality of the hydrogen isotope solutions on the simulation results.	...	10
2.4	Great improvement of the simulation procedure.	...	11
2.5	Concluding remarks.	...	12
	NOTATION	...	13
	REFERENCES	...	14
	Tables and Figures	...	16
3.	CHARACTERISTICS OF H-T SEPARATION COLUMN WITH FEEDBACK STREAM	...	27
3.1	Specific simulation procedure developed.	...	27
3.2	Separation characteristics.	...	29
3.3	Recent progress.	...	30
3.4	Concluding remarks.	...	31
	NOTATION	...	32

REFERENCES	...	32
Tables and Figures	...	33
4. DYNAMICS AND CONTROL	...	39
4.1 Basic control scheme.	...	39
4.2 Parameter setting procedure for the PI controller.	...	40
4.3 Dead time in the measurement transfer function.	...	40
4.4 Stability of the PI control.	...	41
4.5 Concluding remarks.	...	42
NOTATION	...	43
REFERENCES	...	44
Tables and Figures	...	45
5. NEW CASCADE AS A POSSIBLE ALTERNATIVE TO THE TSTA CASCADE	...	54
5.1 Proposal of a new cascade as a possible alternative to the TSTA cascade.	...	54
5.2 Great flexibility to the feed conditions inherent in the new cascade.	...	55
5.3 Concluding remarks.	...	56
REFERENCES	...	57
Tables and Figures	...	58
6. EFFECTS OF HELIUM ON CHARACTERISTICS OF HYDROGEN ISOTOPE DISTILLATION COLUMN	...	64
6.1 Steady state simulation.	...	64
6.2 Dynamic simulation.	...	65
6.3 Concluding remarks.	...	67
NOTATION	...	68
REFERENCES	...	69

Tables and Figures	...	70
7. START-UP ANALYSIS FOR COLUMN CASCADE	...	77
7.1 Significance of a start-up analysis for a cascade composed of multiple columns.	...	77
7.2 Scenarios 1 and 2.	...	77
7.3 Scenario 3.	...	78
7.4 Scenario 4.	...	79
7.5 Concluding remarks.	...	81
REFERENCES	...	81
Tables and Figures	...	82
8. PRELIMINARY EXPERIMENTAL STUDY	...	92
8.1 Significance of HETP and purpose of the experiment.	...	92
8.2 Experimental procedure and the simulation model used.	...	94
8.3 Effect of the vapor velocity on HETP.	...	95
8.4 Comparison among the experimental results for Dixon Ring, Heli-pak, Helix and Coil Pack.	...	97
8.5 Concluding remarks.	...	98
NOTATION	...	98
REFERENCES	...	99
Figures	...	100
ACKNOWLEDGMENT	...	105

## 目 次

1. 序 言	1
1.1 本報の範囲及び意義	1
1.2 本報の概要	4
参考文献	5
図	6
2. 定常シミュレーション	8
2.1 トリチウムシステムにおける水素精留塔のシミュレーション手法	8
2.2 独立変数の初期値の決定法	9
2.3 トリチウムの崩壊熱及び溶液の非理想性がシミュレーション結果に及ぼす影響	10
2.4 シミュレーション手法の大幅な改良	11
2.5 結 言	12
記号表	13
参考文献	14
表及び図	16
3. フィードバック流れを持ったH-T分離塔の特性	27
3.1 特別に開発されたシミュレーション手法	27
3.2 分離特性	29
3.3 最近の進展	30
3.4 結 言	31
記号表	32
参考文献	32
表及び図	33
4. 動特性及び制御	39
4.1 基本的な制御計画	39
4.2 PI調節計に対するパラメーター設定法	40
4.3 測定の伝達関数中のむだ時間	40
4.4 PI制御の安定性	41
4.5 結 言	42
記号表	43
参考文献	44
表及び図	45
5. TSTAカスケードの代替としての1つの新しいカスケード	54
5.1 TSTAカスケードの代替としての1つの新しいカスケードの提案	54

5.2	フィードの条件に対する新カスケードの大きな柔軟性	55
5.3	結 言	56
	参考文献	57
	表及び図	58
6.	ヘリウムが水素精留塔の特性に及ぼす影響	64
6.1	定常シミュレーション	64
6.2	非定常シミュレーション	65
6.3	結 言	67
	記 号 表	68
	参考文献	69
	表及び図	70
7.	塔カスケードのスタートアップに関する解析	77
7.1	多塔システムのスタートアップに関する解析の重要性	77
7.2	シナリオ1及び2	77
7.3	シナリオ3	78
7.4	シナリオ4	79
7.5	結 言	81
	参考文献	81
	表及び図	82
8.	予備的実験	92
8.1	HETPの意味及び実験目的	92
8.2	実験手順及び用いたシミュレーションモデル	94
8.3	蒸気速度のHETPへの影響	95
8.4	ディクソンリング, ヘリパック, ヘリックス, コイルパックに対する 実験結果の比較	97
8.5	結 言	98
	記 号 表	98
	参考文献	99
	図	100
	謝 辞	105

## 1. INTRODUCTION

### 1.1 Scope and significance of the present report

Cryogenic distillation (see Fig. 1.1) is one of the most attractive methods for hydrogen isotope separation : the separation performance is relatively high ; a large flow rate of hydrogen isotopes can be processed ; the system scale is compact ; and the cryogenic operating temperature eliminates the tritium permeation problems. An adequately long packed column can be considered a sort of square cascade composed of a number of separating elements, and it assures high performance. In many cases, multiple columns and equilibrators (catalyst beds) are arranged in cascades to achieve multicomponent separation. Cryogenic distillation is applicable to a number of situations : separation of H, D and T in the mainstream fuel circulation system for a fusion reactor (the feed comprises  $H_2$ , HD, HT,  $D_2$ , DT and  $T_2$ ) ; separation of H and T in the blanket system for the fusion reactor or in the tritium production system ( $H_2$ , HT and  $T_2$ ) ; recovery of tritium from heavy water used in a heavy water reactor (HD,  $D_2$  and DT) ; and concentration of tritium recovered from glovebox atmospheres and other similar sources ( $H_2$ , HD, HT,  $D_2$ , DT and  $T_2$ ). Although France<sup>1)</sup> has much experience in a specific situation of tritium recovery from the heavy water reactor, it is still inadequate to be applied to other situations because of its rather weak theoretical basis. Column cascades handle a variety of feeds, and the input and output specifications for the cascades vary greatly from situation to situation.

In addition, in the mainstream fuel circulation system for the fusion reactor, the feed condition may be greatly variable during the operation. Another fact to be noted is that the radiological standards for tritium lost to the environment are becoming increasingly stricter. Thus, to establish the design, construction, operation and control methods for column cascades for all the situations, systematic and extensive studies are further needed. In those studies, both theoretical and experimental approaches are imperative on various subjects : physico-chemical studies on cryogenic properties of hydrogen isotopes ; development of a set of computer simulation procedures and programs ; detailed analyses on steady state and dynamic column behavior ; laboratory scale experiments measuring fundamental parameters and verifying some of the significant computer predictions ; development of analysis techniques for measuring mole fractions of molecular species with high accuracy, adequately short time and moderate cost ; and operational tests or engineering development for a single, practical scale column and multiple interlinked columns.

Cryogenic hydrogen properties pertinent to fusion technology have been studied mainly by Souers. He has published a very useful report<sup>2)</sup> presenting a significant amount of information on cryogenic hydrogen data. However, properties of HT, DT and T<sub>2</sub> are uncertain and should further be studied. Development of simulation procedures and computer programs has been made mostly by the author. Although a great progress has been made and a number of efficient computer codes are available, the informa-

tion on dynamics and control for column cascades is not adequate yet. Laboratory scale experiments have been performed mainly by Wilkes<sup>3)</sup> and Sherman et al.<sup>4)</sup> They have never reported details on the results, so the dependency of the fundamental parameters (e.g. HETP, flooding velocity) on operational conditions and column specifications is quite uncertain, and the reliability of the briefly described results is not always high. Also, there is a great discrepancy between the values of HETP reported by Wilkes and Sherman. As principal part of the Tritium Systems Test Assembly (TSTA) project, a column cascade of four interlinked columns is under development at Los Alamos (see Fig. 1.2).<sup>4,5)</sup> During this development, the author sincerely hopes that they will make the most of computer simulation work particularly for the start-up of the cascade and the design of more reliable control system.

A goal is to prove long-term operation of column cascades meeting very strict requirements for the products even under great fluctuation of the feed composition. To achieve this goal, we still have to solve many problems or clarify a number of uncertain subjects. The author believes that the computer simulation studies are vitally important in this achievement and, for instance, saves a remarkable amount of experimental effort and the time and cost consumed. The present report gives a critical, brief review of the research results obtained by the author, and the recent development which has not been reported yet. The readers should refer to the original papers cited for more details.

## 1.2 Outline of the present report

In chapters 2 and 3, efficient simulation procedures best suited to hydrogen isotope distillation columns are briefly described, and some of the significant simulation results are also given. The H-T separation column with a feedback stream studied in chapter 3 is highly interesting, and a significant amount of further information is presented. In chapter 4, dynamics and control for a single column are considered and some of the significant simulation results are summarized. Chapter 5 gives a brief description of a column cascade proposed as a possible alternative to the TSTA cascade. In chapter 6, recent simulation results on the effect of helium on column behavior are briefly described. Chapter 7 deals with a start-up analysis for determining a start-up scenario indicating how the full-normal composition profiles are achieved within all the columns. Chapter 8 is the only one where experimental work is treated. The major purpose of the experiment is to study the dependence of HETP on operational conditions and specifications of the packings. Thus, chapters 2, 3 and 5 deal with steady state simulation studies, and chapters 4 and 7 treat dynamic simulation studies. Chapters 6 and 8 include both steady state and dynamic research results.

REFERENCES

- 1) Léger, D., G. Dirian, and E. Roth : *Énergie Nucléaire*,  
12, 135 (1970) (in French).
- 2) Souers, P. C. : UCRL-52628, Lawrence Livermore National  
Lab. (1979).
- 3) Wilkes, W. R. : ERDA-50, 113 (1975).
- 4) Bartlit, J. R., R. H. Sherman, and R. A. Stutz :  
*Cryogenics*, 19, 275 (1979).
- 5) Bartlit, J. R., W. H. Denton, and R. H. Sherman :  
"Hydrogen Isotope Separation," PAT-APPL-037603, US Patent  
Document 4, 353, 871, Oct. 12, 1982.

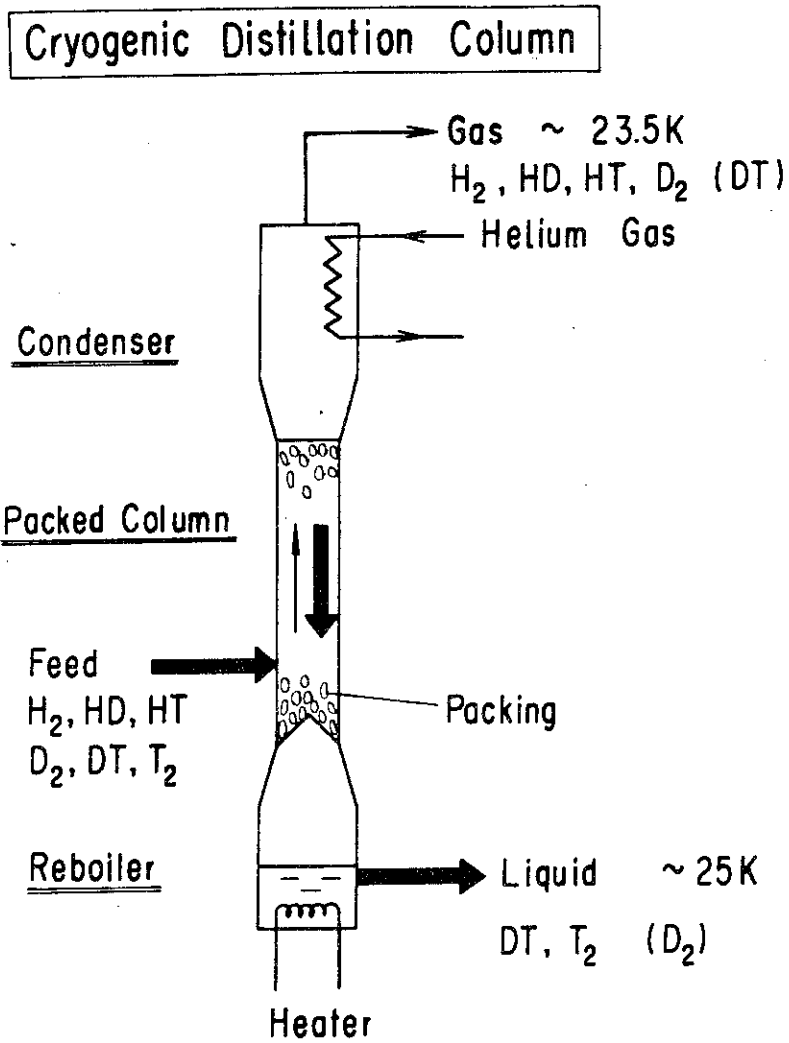


Fig. 1.1 A simplified diagram of a cryogenic distillation column. Helium gas is supplied at  $\sim 19\text{K}$  as the refrigerant at the partial condenser.

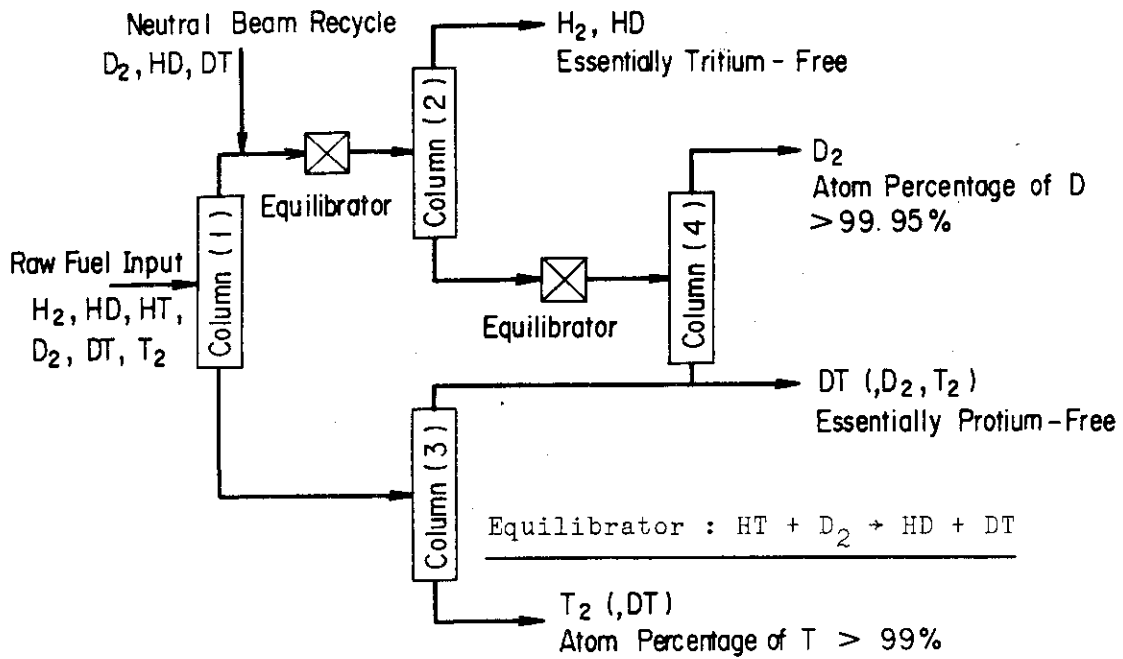


Fig. 1.2 Flow schematic of the column cascade under development for the Tritium Systems Test Assembly (TSTA) at Los Alamos.<sup>4,5)</sup> It simulates a column cascade for hydrogen isotope separation in the mainstream fuel circulation system for a fusion reactor. This column cascade will be evaluated in chapter 5.

## 2. STEADY STATE SIMULATION

### 2.1 A simulation procedure for hydrogen isotope distillation columns in tritium systems

The model column considered is illustrated in Fig. 2.1. The basic equations for solving an operating problem are composed of the overall and component material balances, vapor-liquid equilibrium relationships, stoichiometric equations, and heat balances.<sup>1)</sup> A problem posed is that the number of the unknown variables to be calculated is  $(2m + 3)N$  which is considerably large. For a column processing the six components ( $H_2$ , HD, HT,  $D_2$ , DT and  $T_2$ ) and having eighty stages, for instance, the number is 1200. There are a number of simulation procedures which have been reported for distillation columns in usual chemical engineering systems. Any of the procedures falls into the three categories as explained in Table 2.1. When we try to select one of the procedures, the decision should be made by considering the special features of hydrogen isotope distillation columns in tritium systems : the output specifications required are very strict in most cases ; and the number of stages and reflux ratio are considerably large. Hence, infinitesimal amounts of components are present within the columns. The presence of these components cannot be ignored, and high accuracy is desired for the simulation results for their behavior within the columns. This is particularly true in cases where the infinitesimal amount of component is HT or DT. As explained in Table 2.1, one of the most suitable procedures for finding the solutions

of the basic equations is the Newton-Raphson method where a set of temperatures and liquid flow rates (or equivalently, vapor flow rates) are the independent variables (see Table 2.2).

Namely, after the initial values of temperatures and liquid flow rates are appropriately assumed, their values are repeatedly modified by the Newton-Raphson algorithm until the calculation converges within a prescribed tolerance.

## 2.2 Determination procedures for initial values of the independent variables

It is well known that the convergence characteristics of a Newton-Raphson iterative calculation are greatly dependent on the initial values of the independent variables. In usual cases, the top and bottom temperatures are appropriately assumed, and then the other temperatures are determined by using the assumption of linear variation. The liquid flow rates are determined by neglecting heat balances and using the assumption of equal molal overflows. However, these ways of determining the initial values often fail to present convergence if they are applied to hydrogen isotope distillation columns. Hence, the author<sup>1)</sup> has proposed specific determination procedures.

Column(2) in Fig. 1.2, for instance, has the special feature that the tritium level in the top gas must be extremely low. Hence, the percentage of  $H_2$ -HD in the top gas is almost completely 100 %. The percentage decreases as the stage number increases,

but even on the stage having a large number, the percentage should still be considerably high. Namely, the temperature gradient is expected to be almost flat within the upper part of the column. The author has proposed for such cases method B for determining the initial set of temperatures as illustrated in Fig. 2.2. Some numerical experiments have indicated that method B is very powerful in spite of its simplicity, and it assures rapid achievement of convergence even in cases where the use of method A causes divergence.<sup>1)</sup>

Column(3) in Fig. 1.2, for instance, has a large amount of tritium inventory. In such cases, the phase flow rates within the stripping section decrease greatly owing to the large decay heat effects. Hence, the initial set of liquid flow rates obtained by the assumption of equal molal overflows are far from the solutions, and they often fail to present convergence. The author has proposed an improved procedure as summarized in Table 2.3 where step 6 utilizes the equations derived in Fig. 2.3. It has been proved by numerical experiments using the improved procedure that the number of total iterations needed is not subject to the degree of the tritium decay heat effects.<sup>1)</sup>

### 2.3 Effects of decay heat of tritium and nonideality of the hydrogen isotope solutions on the simulation results

The computational effort is greatly reduced if heat balances are excluded and the ideal form of Raoult's Law is assumed in

the simulation model. However, in cases of considerably high tritium concentration within the column, the incorporation of decay heat is highly significant. As proved in Table 2.4, the neglect of the decay heat causes unacceptable over-estimation of the column performance and reboiler load. As for the  $D_2$ -DT- $T_2$  system, the differences in latent heat of vaporization among the components are practically insignificant. However, for the  $H_2$ -HT- $T_2$  system, they are as significant as the decay heat as shown in chapter 3, because of the larger differences (see Fig. 2.4).

It is well known in physical chemistry that the nonideality of an infinitesimal amount of component is relatively large. Such situations are often found in hydrogen isotope distillation in tritium systems. Above all, the nonideality should be accounted for in predicting the tritium level in the protium waste gas whose accuracy is highly important.

The conclusions described so far have been drawn from the results of a number of numerical experiments.<sup>1)</sup>

#### 2.4 Great improvement of the simulation procedure

The simulation procedure used in the previous sections can be described by the brief flow chart in Fig. 2.5. However, for narrow boiling mixtures<sup>11)</sup> such as hydrogen isotope solutions, there is no need to treat all the basic equations simultaneously and apply the Newton-Raphson algorithm. Hence, the

author<sup>10)</sup> has divided the inner loop in Fig. 2.5 into two loops : the Newton-Raphson loop for the temperature corrections and the successive iteration loop for the flow rate corrections. The order of the Jacobian matrix is thus halved in the Newton-Raphson loop, so the total computation time and computer storage requirement are greatly reduced. The following modification has further been made : the Newton-Raphson method has been replaced by the quasi-Newton method developed by Broyden<sup>12)</sup> where the numerical evaluation of the Jacobian matrix and its inversion are needed only once. The improved procedure thus completed is illustrated in Fig. 2.6. Consequently, the number of total iterations is increased by the replacement, but the total computation time is greatly shortened. When the nonideality of the isotope solutions is incorporated, the corrections of the deviation coefficients are made simultaneously with the flow rate corrections in the outer loop as shown in Fig. 2.6. Some numerical experiments have shown that the total computation time is shortened by almost one order of magnitude by the above-mentioned improvement (see Table 2.5).<sup>10)</sup>

## 2.5 Concluding remarks

An efficient simulation code, CRYDIS-N, has thus been developed. The author will continue to improve CRYDIS-N. Recently, a special subroutine has been added : the tridiagonal matrix algorithm by Wang and Henke<sup>2)</sup> is repeated twice before

proceeding with the calculation illustrated in Fig. 2.6.

The total computation time consumed by the most recent version of CRYDIS-N is also given in Table 2.5.

#### NOTATION

- $B$  = flow rate of bottom product (mol/h)  
 $D$  = flow rate of top product (mol/h)  
 $F_j$  = flow rate of feed stream supplied to  $j$ 'th stage (mol/h)  
 $L_j$  = flow rate of liquid stream leaving  $j$ 'th stage (mol/h)  
 $N$  = number of total theoretical stages (-)  
 $N_F$  = feed stage number (-)  
 $R$  = reflux ratio (-)  
 $T_j$  = temperature on  $j$ 'th stage (K)  
 $U_j$  = flow rate of liquid sidestream from  $j$ 'th stage (mol/h)  
 $V_j$  = flow rate of vapor stream leaving  $j$ 'th stage (mol/h)  
 $W_j$  = flow rate of vapor sidestream from  $j$ 'th stage (mol/h)

$\xi_{i,j}$  = deviation coefficient for accounting for nonideality  
 of hydrogen isotope solutions defined by

$$P_j y_{i,j} = \xi_{i,j} p_{i,j}^* x_{i,j} \quad (2.2)$$

where

- $P_j$  = total pressure on j'th stage (atm)  
 $p_{i,j}^*$  = vapor pressure of i'th component on j'th stage (atm)  
 $x_{i,j}$  = mole fraction of i'th component in liquid stream  
 leaving j'th stage (-)  
 $y_{i,j}$  = mole fraction of i'th component in vapor stream  
 leaving j'th stage (-)

(Subscript)

- $i$  = component index  
 $j$  = stage index

#### REFERENCES

- 1) Kinoshita, M. : "Studies on Simulation Procedures for Stage Processes in Fusion Fuel Cycle and Distillation Systems," Doctoral Dissertation, Kyoto University (1983).
- 2) Wang, J. C. and G. E. Henke : Hydrocarbon Processing, 45, 155 (1966).
- 3) Rose, A., R. F. Sweeny, and V. N. Schrodt : Ind. Eng. Chem., 50, 737 (1958).
- 4) Ishikawa, T. and M. Hirata : Kagaku Kōgaku, 36, 865 (1972) (in Japanese).
- 5) Tomich, J. F. : AIChE J., 16, 229 (1970).
- 6) Boynton, G. W. : Hydrocarbon Processing, 49, 153 (1970).

- 7) Goldstein, R. P. and R. B. Stanfield : Ind. Eng. Chem. Process Des. Develop., 9, 78 (1970).
- 8) Naphtali, L. M. and D. P. Sandholm : AIChE J., 17, 148 (1971).
- 9) Kinoshita, M., I. Hashimoto, and T. Takamatsu : J. Chem. Eng. Japan, 16, 370 (1983).
- 10) Kinoshita, M. : "An Efficient Simulation Procedure Specially Developed for Hydrogen Isotope Distillation Columns," To be published in Fusion Technol.
- 11) Holland, C. D. : "Fundamentals and Modeling of Separation Processes," Printice-Hall Inc., New Jersey (1975).
- 12) Broyden, C. G. : Mathematics of Computation, 19, 577 (1965).
- 13) Souers, P. C. : UCRL-52628, Lawrence Livermore National Lab. (1979).

Table 2.1 Three major categories of previously reported simulation procedures for distillation columns in usual chemical engineering systems.

---

1. Successive Iteration Method

(e.g. tridiagonal matrix method<sup>2)</sup>)

Simple algorithm and computer programming.

Readiness of incorporation of heat balances and nonideality of the solutions.

Poor convergence characteristics in cases of very high column performance.

2. Unsteady Approach<sup>3,4)</sup>

Difficulty of incorporating heat balances.

Unacceptably many time steps needed and long computation time.

3. Newton-Raphson Method<sup>5-9)</sup>

Greater stability and rapid achievement of convergence as long as the initial estimates of the independent variables are good enough.

---

Note : It is reasonable to select a procedure from category 3 for hydrogen isotope distillation columns. Since infinitesimal amounts of components are present, procedures where mole fractions or component flow rates are included in the independent variables should be set aside.<sup>10)</sup>

The author believes that the best method is to choose a set of temperatures and liquid (or vapor) flow rates for the independent variables.

Table 2.2 Nonlinear simultaneous equations to be solved by  
the Newton-Raphson method.

---


$$\begin{array}{l}
 S_1(T_1, \dots, T_N, L_1, \dots, L_N) = 0 \\
 \vdots \\
 S_N(T_1, \dots, T_N, L_1, \dots, L_N) = 0 \\
 E_1(T_1, \dots, T_N, L_1, \dots, L_N) = 0 \\
 \vdots \\
 E_N(T_1, \dots, T_N, L_1, \dots, L_N) = 0
 \end{array}
 \quad \left. \vphantom{\begin{array}{l} S_1 \\ \vdots \\ S_N \\ E_1 \\ \vdots \\ E_N \end{array}} \right\} \quad (2.1)$$

( $T_j$  : temperature,  $L_j$  : liquid flow rate)

---

Note : The selected procedure is a modified version of Tomich's algorithm.<sup>5)</sup> The definition of the S-functions and E-functions is described in his original paper. The Jacobian matrix must numerically be evaluated.

Table 2.3 Determination procedure for the initial set of liquid flow rates.<sup>1)</sup>

- 
- 1) Give the temperature profile (see Fig. 2.2).
  - 2) Give the vapor and liquid flow rates by using the assumption of equal molal overflows.
  - 3) Calculate the liquid mole fractions by the tridiagonal matrix algorithm<sup>2)</sup> and normalize them.
  - 4) Calculate the vapor mole fractions by using the vapor-liquid equilibrium relationships and normalize them.
  - 5) Calculate molar enthalpies of vapor and liquid flows.  
Calculate heat generation rates by decay of tritium.
  - 6) Recalculate the liquid flow rates by using the equations derived in Fig. 2.3. The liquid flow rates thus calculated are used as the initial values.
-

Table 2.4. Comparison among the simulation results obtained by using three different models.

(D<sub>2</sub>-DT-T<sub>2</sub> System)

	Stage	Model I	Model II	Model III
Distribution of liquid flow rate (mol/h)	1	560.0	560.0	560.0
	10	560.0	555.2	527.7
	20	560.0	550.3	489.8
	30	660.0	646.6	551.9
	40	660.0	637.1	507.4
	50	660.0	629.2	457.6
	60	660.0	625.9	405.9
	64	660.0	625.4	385.2
	65	30.0	30.0	30.0
Reboiler load (W)		242	229	127

Note : Model I : heat balances are excluded.

Model II : heat balances are included, but decay heat of tritium is ignored.

Model III : heat balances are fully incorporated including decay heat of tritium.

The three models predict that the purities of the tritium stream from the bottom are 99.4 %, 99.3 % and 98.2 %, respectively. The result by model III is apparently different.

Table 2.5 Comparison between CRYDIS-2 and CRYDIS-N in terms of the total computation time needed (sec).\*)

Column	(1)	(2)	(3)	(4)
CRYDIS-2	25.0	30.0	15.0	21.5
CRYDIS-N	2.79	3.78	1.80	3.71
Most recent version of CRYDIS-N	0.86	0.87	0.61	0.94

Note : The nonideality and heat balances are both incorporated.

The deviation coefficients are estimated by using Souers' procedure.<sup>13)</sup>

CRYDIS-2 and CRYDIS-N are computer codes developed in accordance with the procedures in Fig. 2.5 and Fig. 2.6, respectively.

The four columns in Fig. 1.2 are simulated in this table. The number of total stages is in the range from 65 (column(3)) to 80 (columns(1), (2) and (4)).

The simulation results obtained by means of the two computer codes are identical within the convergence tolerance.

\*) The computer used is the FACOM M-380 SYSTEM at Japan Atomic Energy Research Institute.

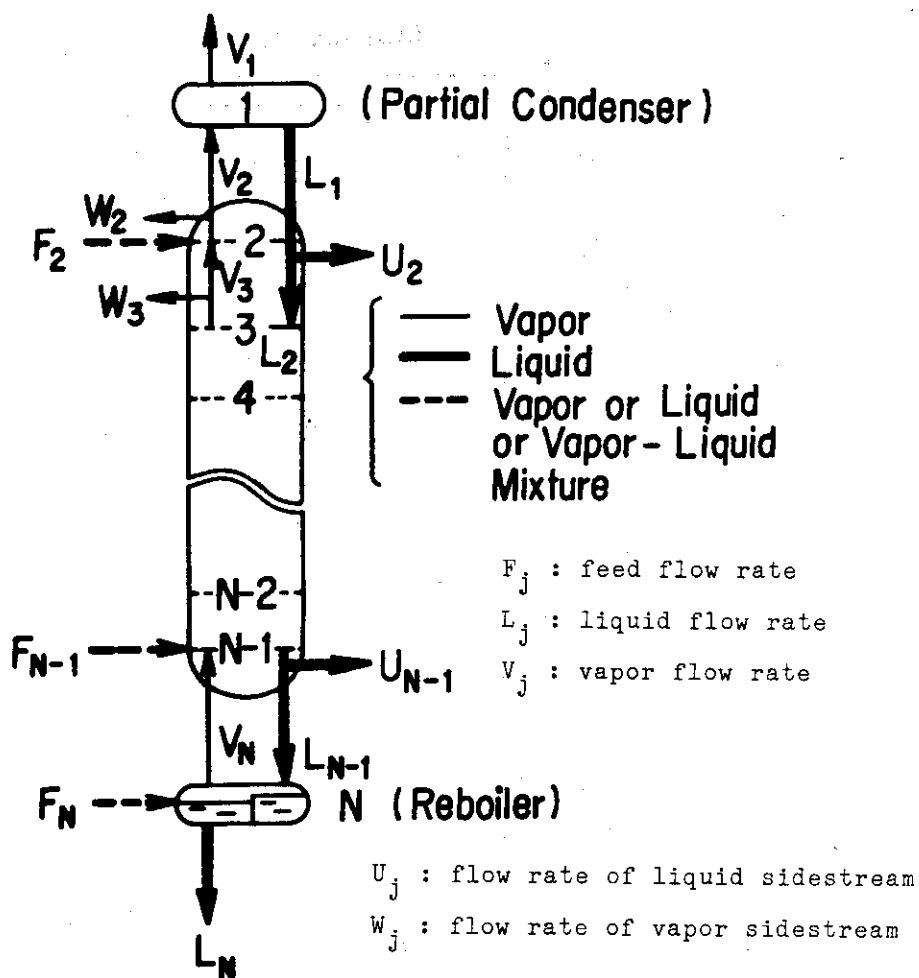


Fig. 2.1 Model column for computer simulation. Provision is made for multiple feeds and sidestreams. The column comprises N theoretical stages. The first stage is the partial condenser and the N'th stage is the reboiler.

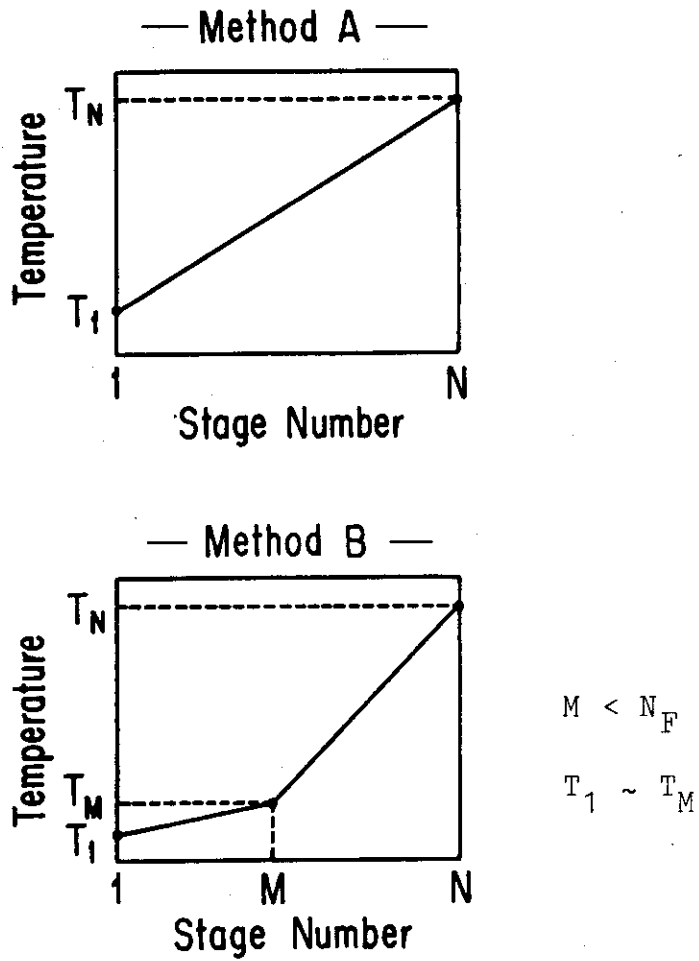


Fig. 2.2 Comparison between the usual method (method A) and the proposed method (method B) for determining the initial set of temperatures. When the specifications required for the bottom product are very strict, method B should be used with  $M > N_F$  and  $T_M \sim T_N$ .

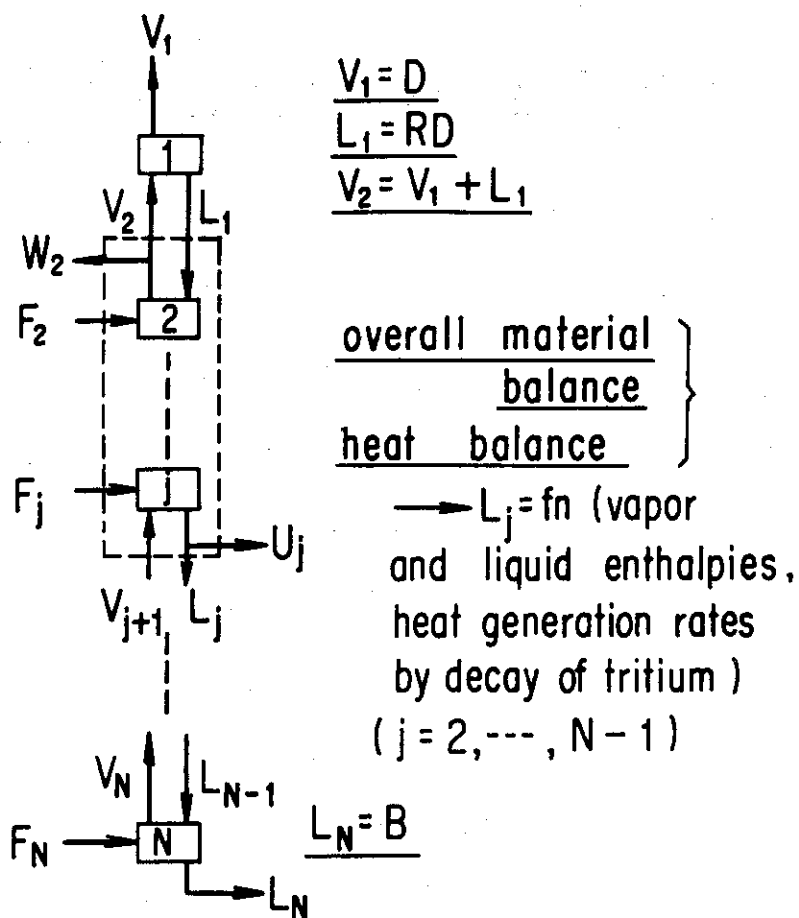


Fig. 2.3 Derivation method of a set of equations used in step 6 in Table 2.3. The overall material balance and heat balance equations around the portion composed of stage 2 through stage  $j$  include  $L_j$  and  $V_{j+1}$ . The derivation is completed by eliminating  $V_{j+1}$  from the two equations.<sup>1)</sup>

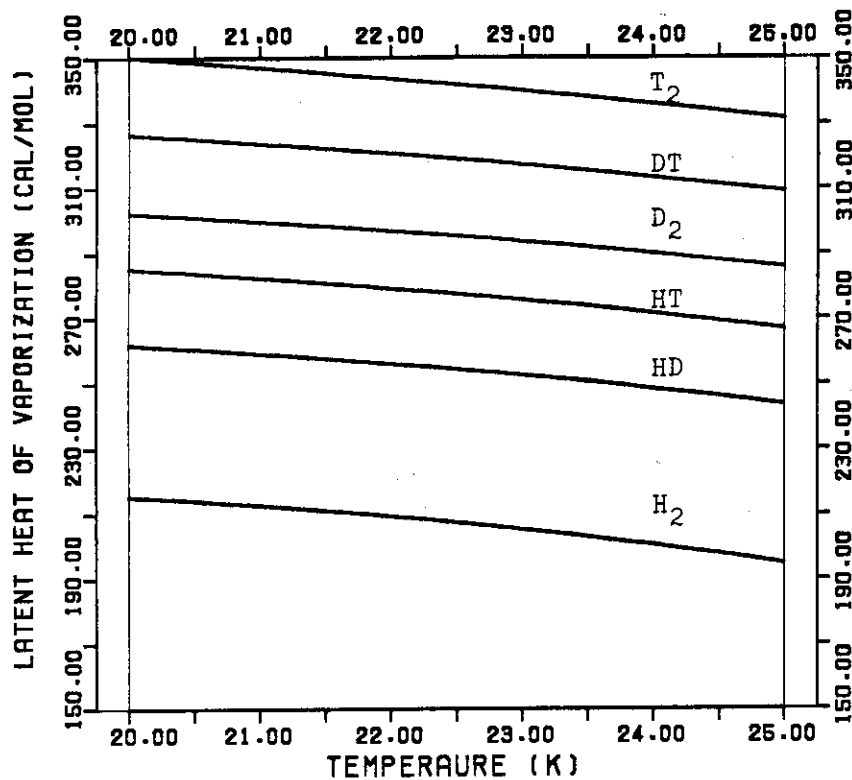


Fig. 2.4 Differences in latent heat of vaporization among the six molecular species of hydrogen isotopes. The vapor and liquid molar enthalpy parameters are given in ref. 6 in chapter 5.

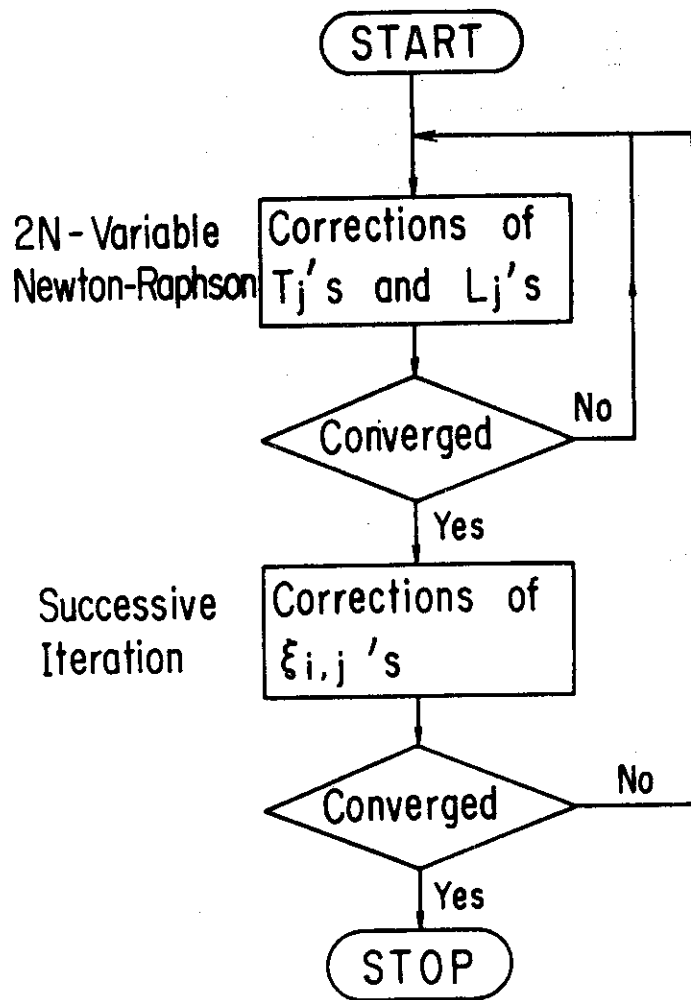


Fig. 2.5 Brief flow chart of the procedure before the improvement. All the basic equations are treated simultaneously. When the nonideality of the isotope solutions are not incorporated, the outer loop is not needed.

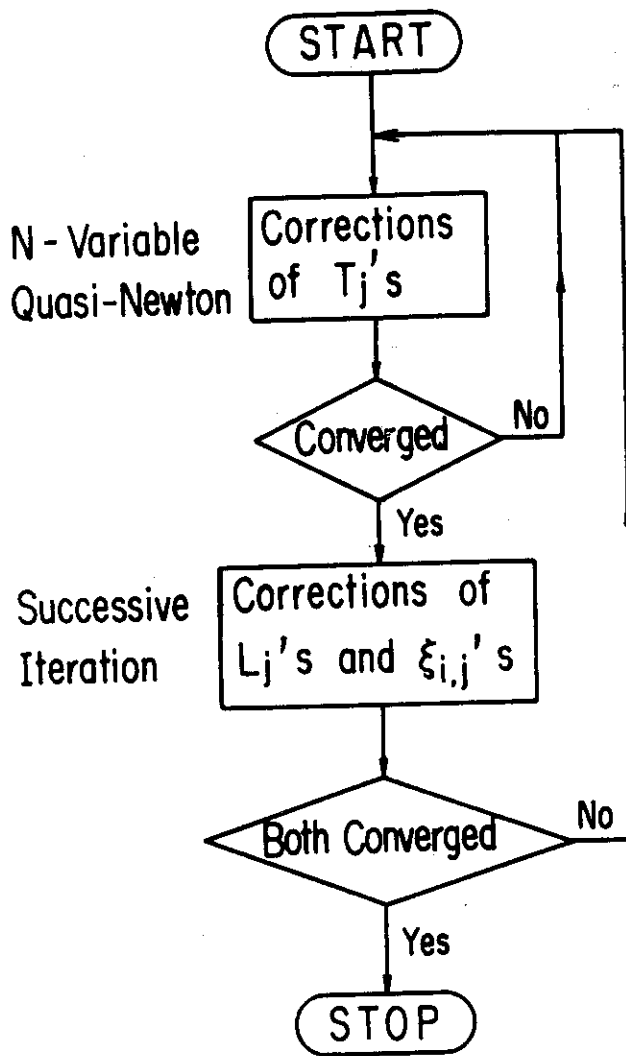


Fig. 2.6 Brief flow chart of the procedure after the improvement. The inner loop treats the component material balances, vapor-liquid equilibrium relationships and stoichiometric equations for the temperature corrections. The outer loop treats the overall material and heat balances for the flow rate corrections.<sup>10)</sup>

### 3. CHARACTERISTICS OF H-T SEPARATION COLUMN WITH FEEDBACK STREAM

#### 3.1 Specific simulation procedure developed

Figure 3.1 shows a flow schematic of an H-T separation column. Because of the presence of HT in the external feed, the complete separation of H and T cannot be achieved by distillation alone. By using an equilibrator, the separation can be accomplished if the sidestream location is appropriate. As shown in Fig. 3.1, a certain amount of HT is fed to the column per unit time, and the same amount of HT is destroyed per unit time in the equilibrator by  $2HT \rightarrow H_2 + T_2$ . A typical composition profile within the column is shown in Fig. 3.2. The role of the computer simulation is to predict the behavior of the key component HT.

The column with the feedback stream has several special features which are not inherent in the columns without the feedback streams. For one thing, the feedback stream poses a serious problem in computer simulation as described below.<sup>1,2)</sup> To simulate the column, the composition of the internal feed is to be given. A method which may readily occur to a mathematical programmer is the following : 1) Assume the atomic fraction of H in the sidestream,  $z_H$  ; 2) calculate the equilibrium composition established by  $H_2 + T_2 = 2HT$  ; 3) calculate the composition profile within the column by using the procedure developed in chapter 2 ; 4) calculate the atomic fraction of H in the sidestream,  $z'_H$  ; and 5) compare  $z'_H$  with  $z_H$ . If  $z'_H$  is almost equal to  $z_H$ , the simulation problem is considered solved. Otherwise, repeat from step 2 after substituting  $z'_H$  into  $z_H$ .

However, a special feature to be emphasized is that  $z'_H$  is very close to  $z_H$  even if  $z_H$  is far from the solution,  $z^*_H$ . If  $z_H$  is much larger than  $z^*_H$ , for instance, the flow rate of H fed to the column is greatly overestimated. Then, the resultant composition profile represents a much larger protium percentage. Thus, the calculated  $z'_H$  is also much larger than  $z^*_H$ , and

$$z_H \sim z'_H . \quad (3.1)$$

Hence, if " $z_H \sim z'_H$ " is used as a convergence criterion, the mole fractions of HT in the two products can have remarkably large errors. The author once considered the function,  $f(z_H)$ , defined by

$$f(z_H) = z_H - z'_H . \quad (3.2)$$

Then, the solution of " $f(z_H) = 0$ " by the Newton method was tested. However, the absolute value of the function proved not to have the unimodality, and the solution process often failed to present convergence. The author has therefore developed another function as illustrated in Fig. 3.3. The material balance for tritium around the column is considered in the figure. As explained in the figure caption, we obtain

$$DY_T + BX_T = B . \quad (3.3)$$

However,  $X_T$  is almost completely equal to unity in most cases, nevertheless  $Y_T$  is infinitesimal. Therefore, Eq.(3.3) cannot be used as a convergence criterion. If  $X_T$  is replaced by  $(1 - X_H)$  in Eq.(3.3), we obtain

$$DY_T - BX_H = 0 . \quad (3.4)$$

Then, the order of magnitude of the two terms in Eq.(3.4) are about the same. By using the approximate equations,  $Y_T = y_{HT}/2$  and  $X_H = x_{HT}/2$ , we obtain

$$h(z_H) = Dy_{HT} - Bx_{HT} = 0 . \quad (3.5)$$

The new function,  $h(z_H)$ , has thus been developed. Equation (3.5) (or equivalently, Eq.(3.4)) is solved by the Newton method. The parameter,  $|(Dy_{HT} - Bx_{HT})/(Dy_{HT})|$ , has very high sensitivity, and represents the very sharp minimum value ( $\sim 0$ ) at  $z_H = z_H^*$ .

Two numerical examples are given in Table 3.1. It is verified that even in cases of  $z_H \sim z_H^*$ , the calculated mole fractions of HT in the products can be quite erroneous. The proposed parameter represents the minimum value very sharply at  $z_H = z_H^*$ . Another useful example is given in Table 3.2. The usual parameter represents extremely low sensitivity, and in the simulation on a digital computer, its value can be even smaller at a worse point of  $z_H$ .

Thus, the problem posed by the presence of the feedback stream has completely been eliminated.

### 3.2 Separation characteristics

Since a simulation program has been completed in accordance with the above-explained method (CRYDIS-N is incorporated as one

of the subroutines), the separation characteristics can be analyzed in detail. Some of the significant results are as follows.<sup>1,2)</sup> The sidestream location has surprisingly large effects on column performance. If the location is not appropriate, high performance cannot be assured even by an excessively large number of stages and high reflux ratio. The flow rate of the sidestream has also large effects. The optimum values of these two key parameters are strongly dependent on the external feed composition and almost independent of the other conditions in usual cases. These results are quite understandable if we recall the requirement that the amount of HT destroyed per unit time in the equilibrators be almost completely equal to the amount of HT fed to the column per unit time.

As for the  $H_2$ -HT- $T_2$  system, the differences in latent heat of vaporization among the components are as significant as decay heat of tritium. If the heat balances are not accounted for, the simulation results are considerably erroneous. Particularly, the reboiler load estimated can be accompanied by a remarkable error exceeding + 250 %.

### 3.3 Recent progress

The variables to be kept as low as possible are the levels of tritium and protium in the top gas and in the bottom liquid, respectively. To keep both of the two variables adequately low by the smallest possible number of stages and reflux ratio,

it may be profitable to set the flow rate of the bottom stream ( $= B$ ) at a value different from  $F_{ex}Z_T$ . Hence, the second equation in Fig. 3.3 has recently been changed to

$$F_{ex}Z_T = \eta B . \quad (3.6)$$

Then, the equation to be satisfied is

$$DY_T - BX_H = B(\eta - 1) . \quad (3.7)$$

The function to be zeroed is expressed by

$$h(z_H) = DY_T - BX_H - B(\eta - 1) . \quad (3.8)$$

The equation,  $h(z_H) = 0$ , is solved without using the approximate equations,  $Y_T = y_{HT}/2$  and  $X_H = x_{HT}/2$ . Thus, the column can be simulated under a variety of input and output specifications.

#### 3.4 Concluding remarks

A computer code, CRYDIS-B, is available to simulate the column shown in Fig. 3.1. The author will continue to improve CRYDIS-B. The computation time needed to simulate the column under the conditions given in Table 3.3 by using the most recent version of CRYDIS-B (by incorporating heat balances and the nonideality) is 2.91 sec.

## NOTATION

- $B$  = flow rate of bottom product (mol/h)  
 $D$  = flow rate of top product (mol/h)  
 $F_{ex}$  = flow rate of external feed stream (mol/h)  
 $X_H$  = atomic fraction of H in bottom product (-)  
 $X_T$  = atomic fraction of T in bottom product (-)  
 $x_{HT}$  = mole fraction of HT in bottom product (-)  
 $Y_T$  = atomic fraction of T in top product (-)  
 $y_{HT}$  = mole fraction of HT in top product (-)  
 $Z_T$  = atomic fraction of T in external feed stream (-)  
 $z_H$  = input value of atomic fraction of H in sidestream for  
main distillation calculation (-)  
 $z'_H$  = output value of atomic fraction of H in sidestream from  
main distillation calculation (-)  
 $z^*_H$  = correct value of  $z_H$  (-)

## REFERENCES

- 1) Kinoshita, M. : "Studies on Simulation Procedures for Stage Processes in Fusion Fuel Cycle and Distillation Systems,"  
Doctoral Dissertation, Kyoto University (1983).
- 2) Kinoshita, M. and Y. Naruse : Nucl. Technol./Fusion,  
2, 410 (1982).

Table 3.1 Numerical examples proving that the results can be quite erroneous unless  $z^*_H$  is very accurately found.<sup>1)</sup>

Case	$z_H$	$y_{HT}$	$x_{HT}$	$ Dy_{HT} - Bx_{HT} /(Dy_{HT})$
1	0.33500	0.1041E-1	0.1177E-3	0.898
	<u>0.33835</u>	0.1108E-2	0.1234E-3	0.00235
	0.33857	0.8822E-3	0.1236E-3	0.261
2	0.50000	0.3244E-3	0.6254E-5	0.826
	0.60663	0.7893E-4	0.7054E-5	0.196
	<u>0.61567</u>	0.7297E-4	0.8103E-5	0.000589
	0.61857	0.7120E-4	0.1912E-4	1.42

Note : The value underlined represents  $z^*_H$ .

In case 2, for example,  $z'_H = 0.50003$  in the case of  $z_H = 0.50000$  and  $z'_H = 0.61856$  in the case of  $z_H = 0.61857$ .

Table 3.2 Numerical example proving the high sensitivity of the proposed parameter.

$z_H$	Usual parameter $(z_H - z_H^i)/z_H$	Proposed parameter $(Dy_{HT} - Bx_{HT})/(Dy_{HT})$
0.500000	1.24E-7	- 3.47E-1
0.463375	4.71E-7	8.01E-2
0.470372	3.87E-7	4.52E-3
0.470782	3.82E-7	- 5.17E-6
0.470782*	3.82E-7	2.30E-6

\*) Converged within the prescribed tolerance.

Note : This table gives an iteration history of the Newton procedure for solving  $h(z_H) = 0$  where the solution  $z_H^*$  is successfully found. The usual parameter remains essentially unchanged during the iteration.

Table 3.3 Design specifications for the H-T separation column.

---

Flow rate of external feed = 10 mol/h  
 Atom fraction of tritium in external feed = 0.9  
 Number of total stages = 80  
 External feed stage number = 40  
 Sidestream stage number = 25  
 Internal feed stage number = 30  
 Flow rate of top product = 0.995 mol/h  
 Reflux ratio = 50  
 Flow rate of vapor sidestream = 15 mol/h  
 Operating pressure = 1 atm  
 Heat subtraction of 200 cal/h (per stage) is made on stages 41  
 through 79.

---

Compositions of input and output streams :

---

	H <sub>2</sub>	HT	T <sub>2</sub>
External feed	0.1434E-1	0.1713	0.8143
Top product	1.0000	0.1553E-6	0.2619E-15
Bottom product	0.8872E-17	0.1111E-2	0.9989

---

Flow rate of tritium lost from the top ~ 40 Ci/y  
 Protium percentage in bottom product ~ 0.05 atom%  
 Condenser load = 12.4 W  
 Reboiler load = 20.8 W  
 Required refrigeration capacity (excluding heat leak) = 21.5 W.

---

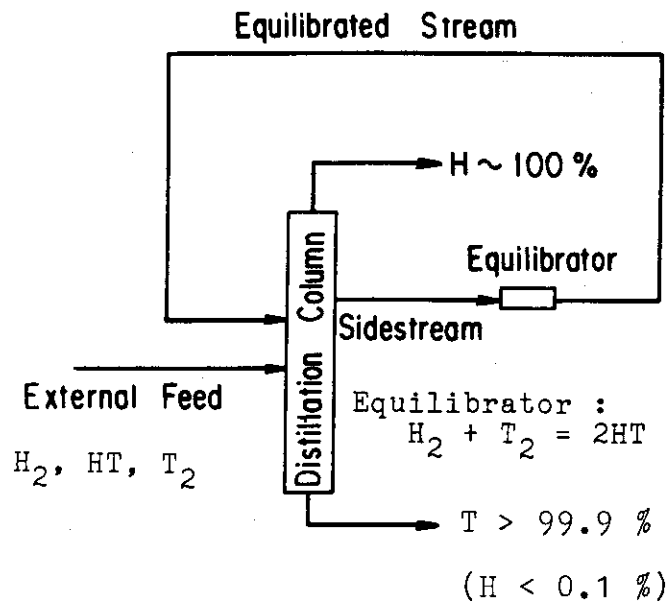


Fig. 3.1 Flow schematic of an H-T separation column with a feedback stream. The vapor sidestream abundant in HT is withdrawn and transferred to the equilibrator. The equilibrated stream recycled to the column is called 'internal feed'. Such columns are needed for removing protium from the H-T mixture in the breeder blanket system and tritium production system for the fusion reactor.

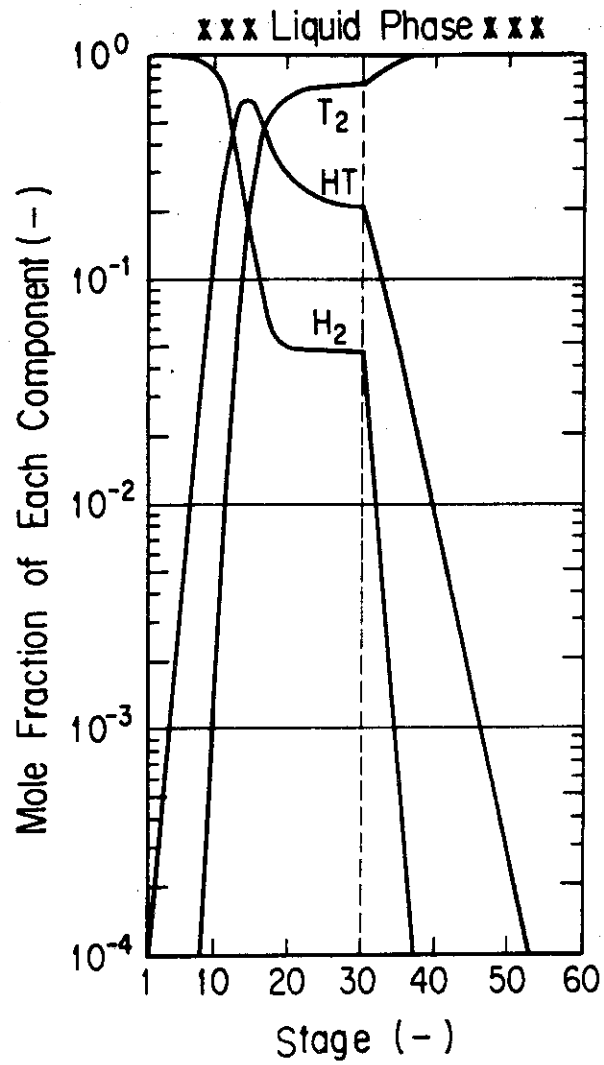
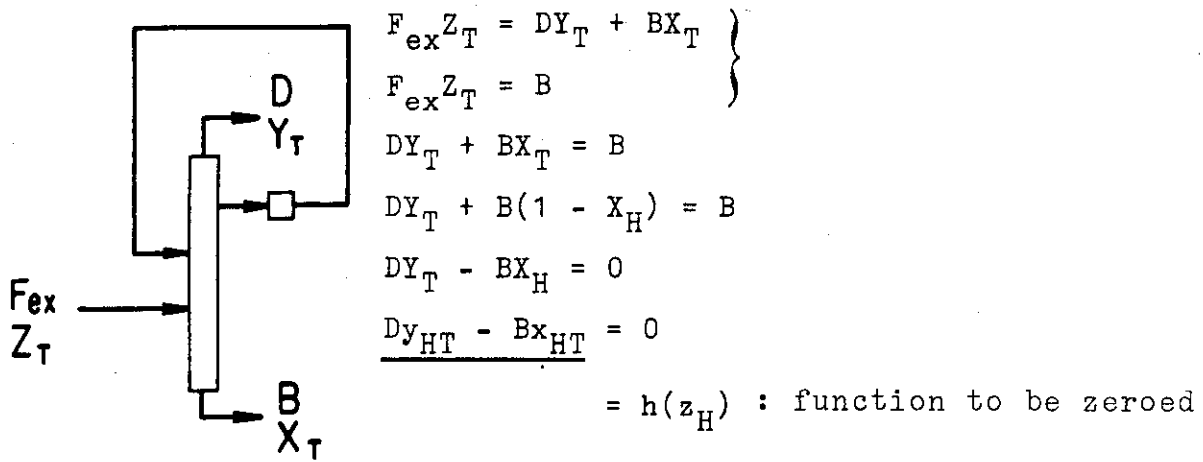


Fig. 3.2 Typical composition profile within the H-T separation column. It should be noted that HT represents an interesting profile.



$$|(Dy_{HT} - Bx_{HT}) / (Dy_{HT})| < \epsilon, \quad 0 < \epsilon \ll 1 : \text{convergence criterion}$$

Fig. 3.3 Development of a new function to be zeroed.

For complete separation of H and T, the flow rates of the two products are established so that the following condition can be satisfied :  $F_{ex} Z_T = B$ . The third equation is obtained by eliminating  $F_{ex} Z_T$  from the first and second equations.

## 4. DYNAMICS AND CONTROL

### 4.1 Basic control scheme

To discuss a basic control scheme for a single column, column(1) in Fig. 1.2 is chosen as an example. The composition profile within the column is shown in Fig. 4.1. The four species,  $H_2$ , HD, HT and  $D_2$ , are recovered at the top, and the other species, DT and  $T_2$ , are recovered at the bottom.

The basic control scheme proposed by Evans et al.<sup>1)</sup> is illustrated in Fig. 4.2. The variables to be monitored as measures of column performance are mole fractions of DT in the top gas and  $D_2$  in the bottom liquid. In this case, the mole fraction of DT in the top gas is considered the primary controlled variable. The manipulated variable is the flow rate of the top gas. The column pressure and the liquid level in the reboiler are controlled by the heat removal rate at the condenser and the flow rate of the bottom liquid, respectively. The heat addition rate at the reboiler is maintained proportional to the feed flow rate. Thus, the column performance is kept constant even under variations in the feed conditions. The principal concern is how to manipulate the top gas flow rate against the mole fraction of DT in the top gas. The other controls are assumed to act instantaneously. The mole fraction of DT and the top gas flow rate are referred to as the controlled variable and the manipulated variable, respectively.

Based on the control scheme in Fig. 4.2, the author<sup>2-4)</sup> has studied the characteristics of the control operation. First,

the two responses of the controlled variable were calculated to a step increase in the DT mole fraction in the feed and to a step decrease in the manipulated variable. The results showed that the mean delay time of the former response was significantly longer than that of the latter response. Hence, the feedback control seemed adequate. Figure 4.3 shows a block diagram of the negative feedback control scheme proposed. As illustrated in the figure,  $G_p(s)$  can be considered the first order lag system. According to the calculation results by the author,  $\tau/T_p$  is adequately smaller than unity. In such cases, the proportional-integral (PI) control is known to be successful. The dead time in  $G_m(s)$  will be discussed in detail later.

#### 4.2 Parameter setting procedure for the PI controller

The two PI controller parameters, proportional sensitivity and integral time, can be determined by investigating the roots of the characteristic equation for the block diagram shown in Fig. 4.3. The parameter setting procedure proposed by the author is summarized in Table 4.1.

#### 4.3 Dead time in the measurement transfer function

For distillation columns in general chemical systems, the condenser temperature can be used as a measure of the top

composition under a successful pressure control. For a hydrogen isotope distillation column, however, such methods are impractical, because no appreciable change in the condenser temperature occurs even if the DT mole fraction at the top becomes unacceptably high. Hence, an analytical device must be used for the direct measurement of the controlled variable. The total time delay ( $= \tau_m$ ) in the measurement can be considered to represent the time required to sample the gas and perform the analysis, if the time needed to get the signal to the controller is negligibly short. If the device gives a continuous reading after the delay, the dead time in  $G_m(s)$  is equal to  $\tau_m$ . However, many of the devices (e.g. gas chromatography) give the analytical results at discrete times: the sample must be held until the subsequent measurement is available. As illustrated in Fig. 4.5, the dead time is to be increased by a factor of about 1.5 in such sample-and-hold operations. Since the dead time is the key parameter affecting the stability of the PI control to a large extent, the relation,  $\tau \sim 1.5\tau_m$ , is highly significant.

#### 4.4 Stability of the PI control

Once  $\tau_m$  is known, the two PI parameters can be specified for a successful operation by following the procedure summarized in Table 4.1. Figure 4.6 shows the response of the controlled variable to a step change in the feed composition under no control, and Fig. 4.7 shows the same response under a PI control.<sup>3,4)</sup>

If the PI parameters are inappropriate, the great instability can be caused as shown in Fig. 4.8.

Thus, a procedure is now available to set the two PI parameters avoiding instability and proportional-only control behavior.

#### 4.5 Concluding remarks

All the calculations have been made by neglecting heat balances and assuming Raoult's Law and constant molal holdup specifications. Namely, a set of ordinary differential equations have been solved by using the Improved Euler method.<sup>2,3)</sup> The author believes that this simple model is adequate to grasp basic characteristics of the control operation. Unlike in cases of steady state simulation, quantitatively accurate results are very difficult to obtain even by a more complicated model, owing to the usual assumption that the vapor leaving a stage is in equilibrium with the liquid leaving that stage at any time. Also, the hydraulic effects are difficult to account for in the model. Hence, the author will continue to use the simple model for the time being.

However, a computer program (CRYDIS-RDS) in which heat balances, nonideality and constant volume holdup specifications are incorporated has already been completed.<sup>3,5)</sup> Thus, the author is ready to analyze the effects of these factors on the dynamic simulation results. Unless the complicated model gives results

qualitatively different from the results by the simple model, the author will not use the complicated model.

The most significant subject to be studied in the near future is to extend the dynamic simulation to a column cascade composed of multiple interlinked columns. However, a great deal of computational effort will be needed. The first thing to do is therefore to modify the computer code, CRYDIS-D, for shortening the computation time. The author is now testing several numerical integration techniques other than the Improved Euler method (e.g. Milne method, Adams-Moulton method, Runge-Kutta-Gill method, etc.), and developing a more efficient simulation code.

#### NOTATION

$K$  = proportional sensitivity (h/mol)

$T_i$  = integral time (h)

$T_p$  = time constant in process transfer function (h)

$y_{DT,1}$  = mole fraction of DT in top gas (-)

$\tau$  = dead time in measurement transfer function (h)

$\tau_m$  = time delay in gas analysis (h)

## REFERENCES

- 1) Evans, L. B., B. Joseph, and F. Ziegler : "Simulation Study of the Isotope Separation System for the Tritium Systems Test Assembly at Los Alamos Scientific Laboratory," Massachusetts Institute of Technology, Private Communication (1979).
- 2) Kinoshita, M. and Y. Naruse : J. Nucl. Sci. Technol., 18, 595 (1981).
- 3) Kinoshita, M. : "Studies on Simulation Procedures for Stage Processes in Fusion Fuel Cycle and Distillation Systems," Doctoral Dissertation, Kyoto University (1983).
- 4) Kinoshita, M., J. R. Bartlit, and R. H. Sherman : Nucl. Technol./Fusion, 5, 30 (1984).
- 5) Kinoshita, M. and Y. Naruse : JAERI-M 9657, Japan Atomic Energy Research Institute (1981).

Table 4.1 Parameter setting procedure for the PI controller.<sup>2-4)</sup>

- 
1. Calculate responses of the controlled variable assuming several different magnitudes of step changes in the manipulated variable.
  2. Determine the process transfer function,  $G_p(s)$ . The parameters in  $G_p(s)$  are given as functions of the magnitude assumed in step 1.
  3. Determine the open loop transfer function,  $G_c(s)G_p(s)G_m(s)$ , and investigate the roots of the characteristic equation.
  4. Set the PI controller parameters avoiding the instability and the behavior of the proportional-only control.
- 

Note : The major point of the procedure is that it accounts for the strong nonlinearity of the column to some extent inspite of its simplicity.

{ Number of Total Theoretical Stages = 80  
 { Feed Stage Number = 50  
 { Reflux Ratio = 25  
 {  $\frac{\text{Top Product Flow Rate}}{\text{Feed Flow Rate}} = 0.25$

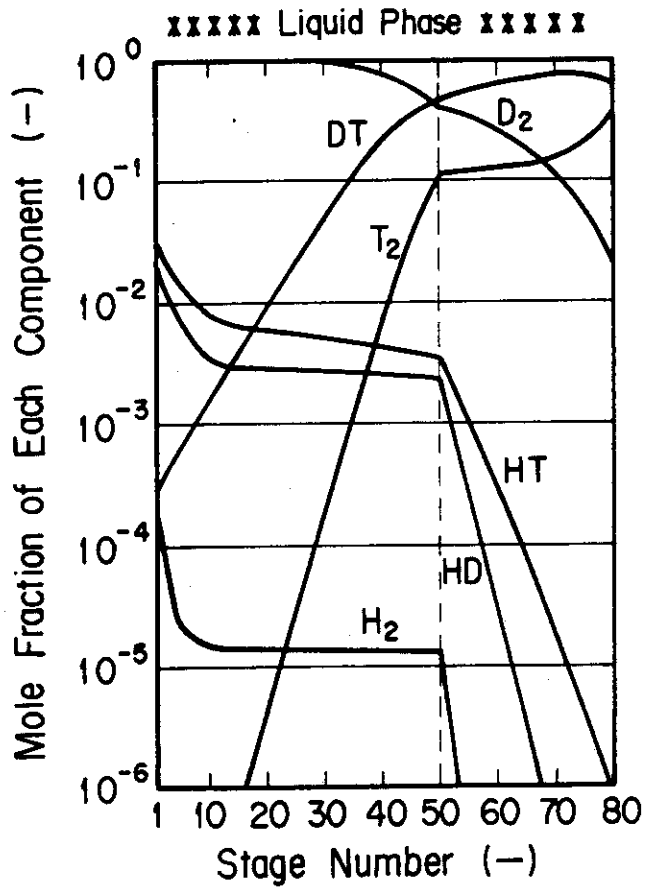


Fig. 4.1 Composition profile within column(1) in Fig. 1.2 under the full-normal condition.

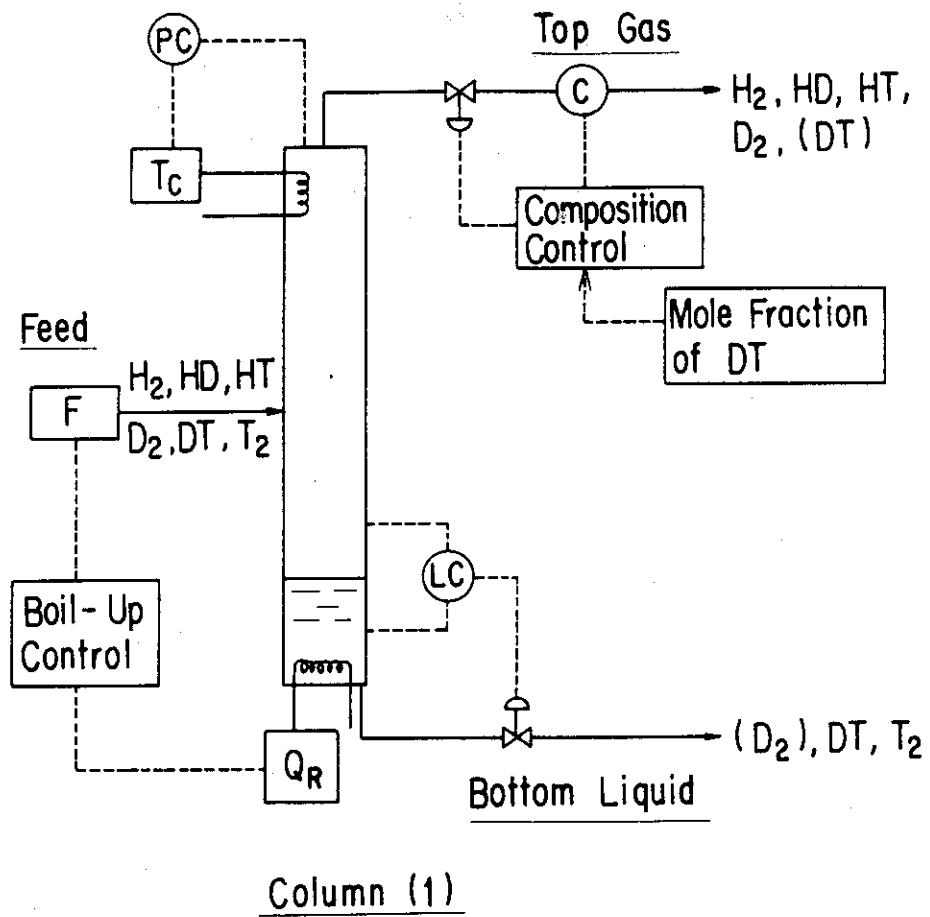
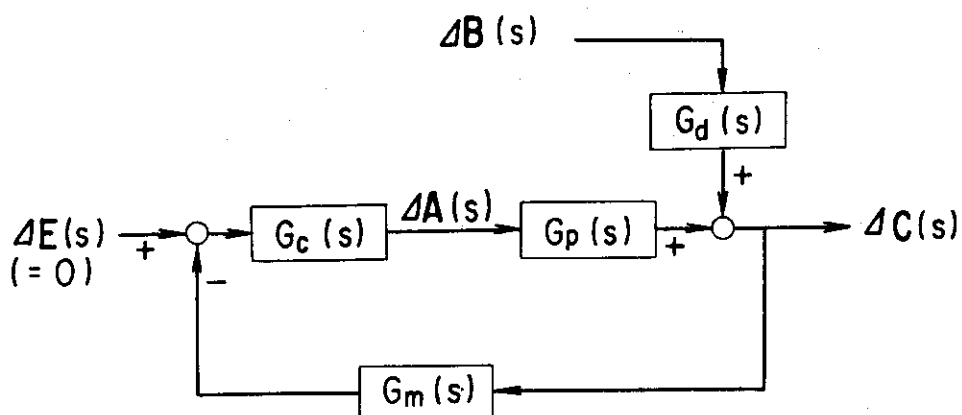


Fig. 4.2 Basic control scheme proposed by Evans et al.<sup>1)</sup>  
 By using this scheme, the author has analyzed  
 the control characteristics.



A : Manipulated Variable      B : Disturbance  
 C : Controlled Variable      E : Reference  
 $G_c$  : Controller Transfer Function  
 $G_d$  : Disturbance Transfer Function  
 $G_m$  : Measurement Transfer Function  
 $G_p$  : Process Transfer Function

Fig. 4.3 Block diagram of a negative feedback control scheme considered. The two transfer functions,  $G_p(s)$  and  $G_m(s)$ , are the first order lag system and the dead time system, respectively. The proportional-integral (PI) action is chosen for  $G_c(s)$ . The most significant disturbance is fluctuation or variation of the feed composition.

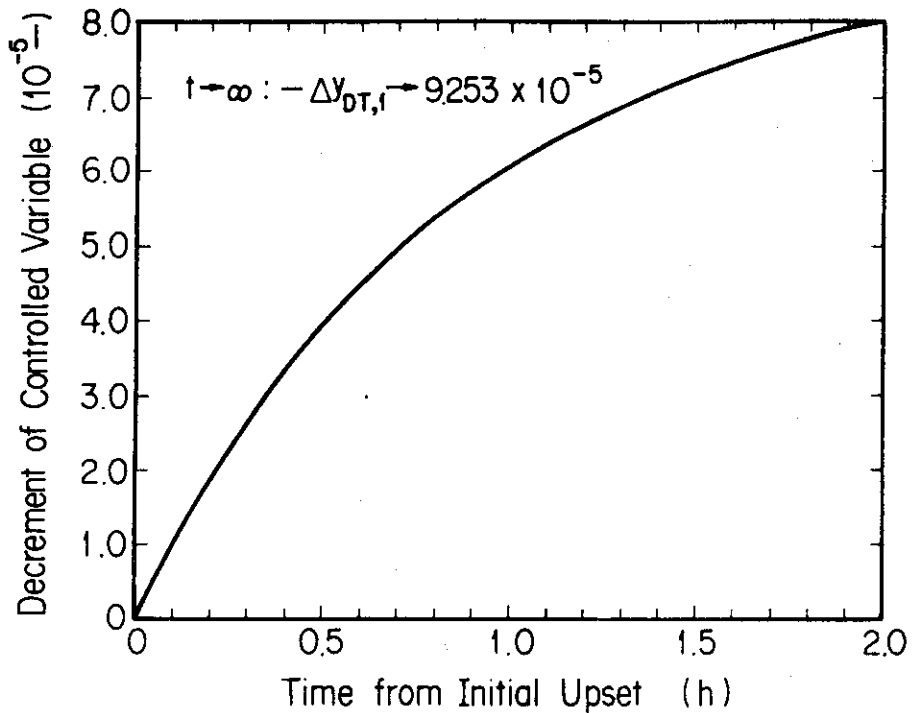


Fig. 4.4 Response of the controlled variable (mole fraction of DT in the top gas) to a step decrease in the manipulated variable (flow rate of the top gas). An example is given here. The curve has no inflection point, and the dead time is zero. Hence, the process transfer function,  $G_p(s)$ , can be considered a first order lag system. It should be noted that the hydraulic effect is assumed to be negligible. More details are described in refs. 3 and 5.

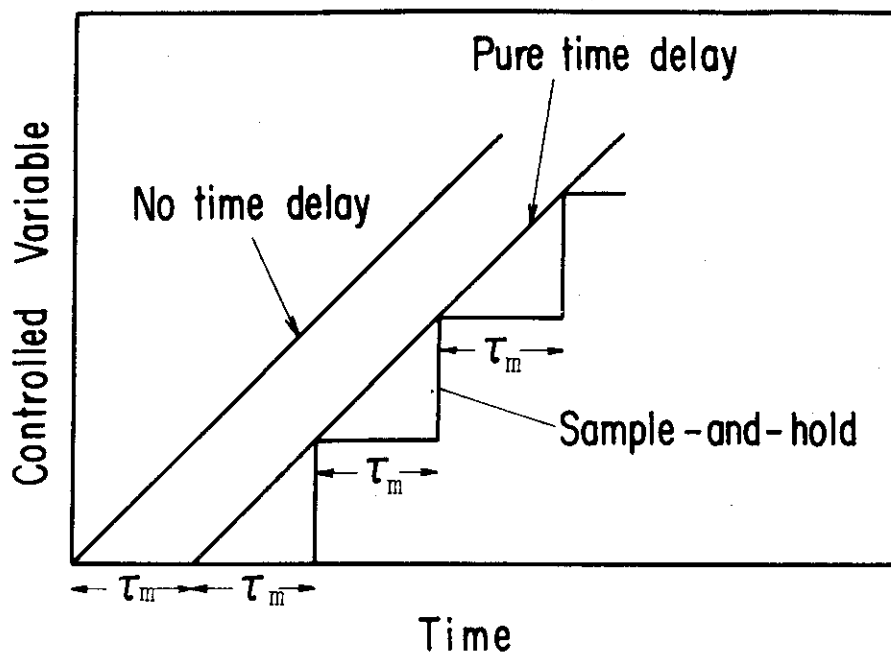


Fig. 4.5 Three typical cases in the observation of the controlled variable. Assume that the controlled variable changes as the line, 'No time delay'. If the analytical device gives a continuous reading with no time delay, the exact line is observed. If it gives a continuous reading after the time delay  $\tau_m$ , the line, 'Pure time delay', is observed. If it gives the analytical results discretely, the line, 'Sample-and-hold', is observed.

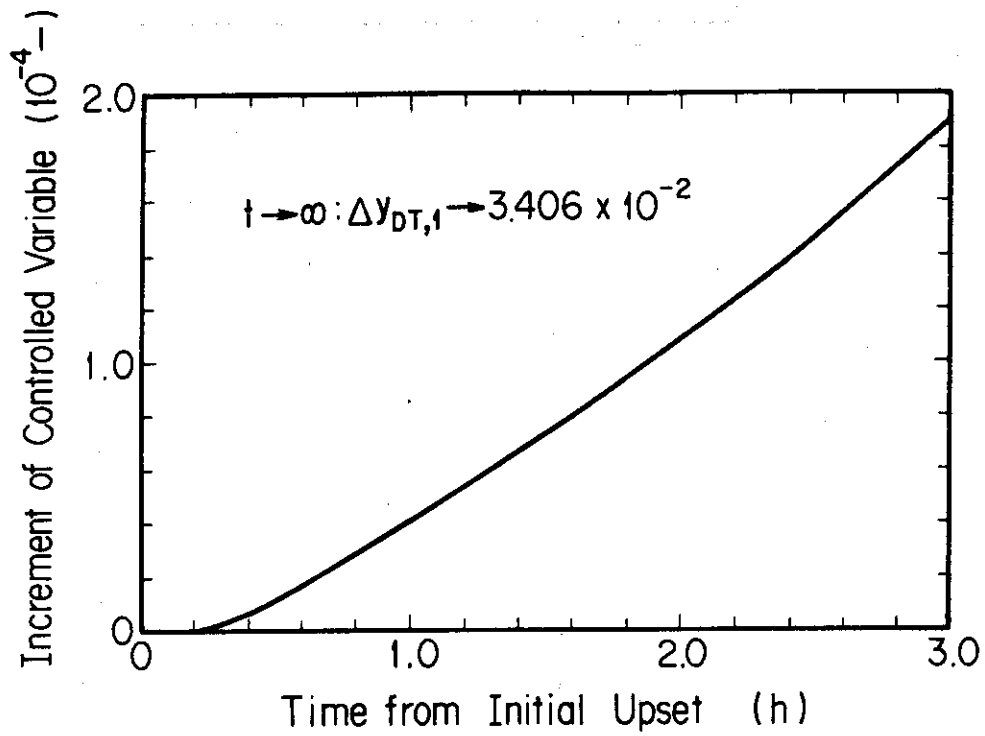


Fig. 4.6 Response of the controlled variable to a step increase in the mole fraction of DT in the feed. The PI control operation is not performed. An example is given here. More details are described in refs. 3 and 5.

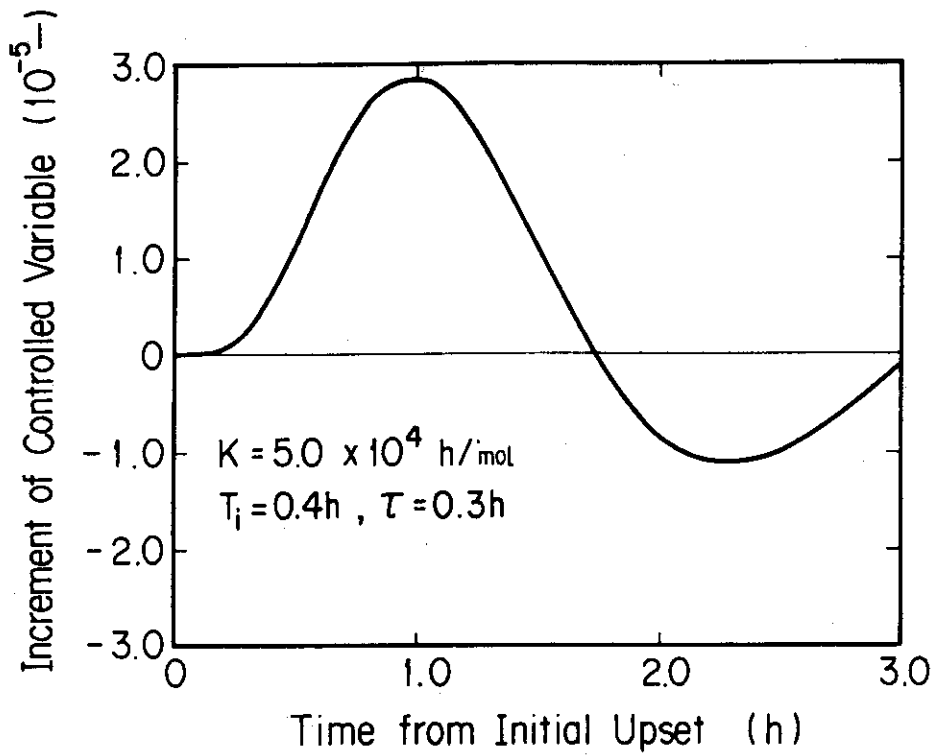


Fig. 4.7 Response of the controlled variable calculated under the condition in Fig. 4.6 with the exception that a PI control operation is performed. The two PI controller parameters are determined in accordance with the procedure explained in Table 4.1. An oscillatory line which is damped with the time increase is obtained, and the control is successful.

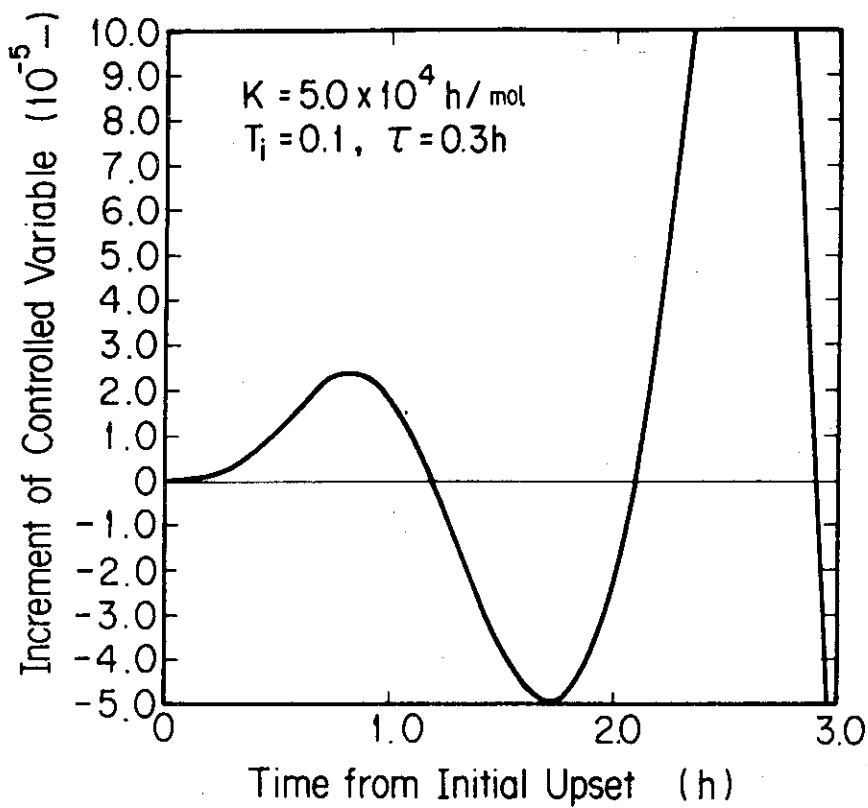


Fig. 4.8 Another example under a PI control where the controller parameters are inappropriate. Since the integral time is too small, great instability is caused. This figure should be compared with Fig. 4.7.

## 5. NEW CASCADE AS A POSSIBLE ALTERNATIVE TO THE TSTA CASCADE

### 5.1 Proposal of a new cascade as a possible alternative to the TSTA cascade

The cryogenic distillation column cascade shown in Fig. 1.2 is a typical cascade in the mainstream fuel circulation system for a fusion reactor.<sup>1)</sup> Another cascade developed at Argonne National Laboratory<sup>2,3)</sup> is shown in Fig. 5.1. They assume rather small numbers of total stages and reflux ratios for the columns, so the performance is not adequately high. By increasing those parameters, much higher performance could be obtained, but in any case the cascade does not produce a pure tritium stream. The cascade has no appreciable advantage compared with the TSTA cascade.

Before describing the new cascade, some information is given on a column with a feedback stream shown in Fig. 5.2. It processes the six molecular species of hydrogen isotopes.<sup>4,5)</sup> A certain amount of HT is fed to the column per unit time, and the same amount of HT is destroyed per unit time in the equilibrators by  $HT + D_2 \rightarrow HD + DT$ . Thus,  $H_2$  and HD are recovered at the top, and  $D_2$ , DT and  $T_2$  are recovered at the bottom. A typical composition profile within the column is shown in Fig. 5.3.

By using the above-mentioned separation column as the lead column, the author<sup>6)</sup> has developed a new cascade shown in Fig. 5.4. A comparison between the new cascade and the TSTA cascade is made in Table 5.1. Apparently, no great advantage of the new cascade can be found just from the table. Its attractive feature will be

described in the next section.

## 5.2 Great flexibility to the feed conditions inherent in the new cascade

As for the TSTA cascade, an adequately large flow rate of deuterium stream as the NBI recycle plays a very important role in decreasing the HT mole fraction in the feed to column(2) to an adequately low value. As a consequence, both an adequately low tritium level in the top gas from column(2) and a highly pure deuterium stream from the top of column(4) can successfully be obtained. However, the flow rate of the NBI recycle depends on the design of the NBI device. There is no guarantee of such an adequately large flow rate. If the flow rate is not adequate, the cascade configuration must be changed as shown in Fig. 5.5. On the other hand, some numerical experiments by the author<sup>6)</sup> have shown that the performance of the new cascade is not subject to the flow rate of the NBI recycle : the same performance can be assured even if as an extreme case there is no NBI recycle stream, just by adjusting the top, sidestream and bottom flow rates with the other parameters unchanged.

As shown in Figs. 1.2 and 5.4, the protium percentage in the raw fuel input was assumed to be 1 %. However, this value is more or less uncertain. Assume, for instance, that the percentage is changed to 3 %. Simulation results for the TSTA cascade have indicated that the condenser load for column(2) must be about

1.5 times larger to assure the same performance. That is, the vapor flow rate within column(2) and its inner diameter are also required to be larger. This requirement is acceptable to a column cascade which is going to be built, but unacceptable to a cascade which has already been built. On the other hand, the new cascade accommodates 3 % H in the raw fuel input only if the top, sidestream and bottom flow rates are adjusted.<sup>6)</sup>

Thus, the new cascade presents great flexibility to the feed conditions.

### 5.3 Concluding remarks

A computer code, CRYDIS-R, is available to simulate the columns in Fig. 5.4. The simulation procedure is described in refs. 4 - 6. The two columns have 120 stages. The computation time needed in a typical case is 5.37 sec for column(1) and 7.92 sec for column(2). The author have dealt mainly with the TSTA cascade so far, but is now much more interested in the new cascade. Significant subjects for further study are analyses on control characteristics of the cascade and on the start-up scenarios (refer to chapter 7).

## REFERENCES

- 1) Bartlit, J. R., R. H. Sherman, R. A. Stutz, and W. H. Denton :  
Cryogenics, 19, 275 (1979).
- 2) Misra, B. and V. A. Maroni : Nucl. Technol., 35, 40 (1977).
- 3) Davis, J. F. et al. : Nucl. Technol., 46, 149 (1979).
- 4) Kinoshita, M. : JAERI-M 82-047, Japan Atomic Energy Research  
Institute (1982).
- 5) Kinoshita, M. : "Studies on Simulation Procedures for Stage  
Processes in Fusion Fuel Cycle and Distillation Systems,"  
Doctoral Dissertation, Kyoto University (1983).
- 6) Kinoshita, M. : "A Cryogenic Distillation Column Cascade  
for a Fusion Reactor," To be published in Fusion Technol.
- 7) Bartlit, J. R., W. H. Denton, and R. H. Sherman : Proc. 3rd  
Topical Mtg. on Technol. of Controlled Nucl. Fusion,  
Santa Fe, NM, May 9 - 11, 1978, pp. 778 - 783.
- 8) Sherman, R. H. : "The Isotope Separation System," Private  
Communication, Los Alamos National Lab. (1983).

Table 5.1 Comparison between the TSTA cascade and the new cascade proposed.<sup>6)</sup>

	TSTA cascade	Present cascade
Total refrigeration capacity required	143 W	143 W
Total tritium inventory	62 g	96 g
Packed height of the highest column	4.25 m	5.9 m
Flow rate of tritium lost from cascade	25.0 Ci/y	23.7 Ci/y
Purity of deuterium stream	99.96 %	99.96 %
Purity of tritium stream	99.21 %	99.22 %

Note : The HETP value and vapor velocity chosen are assumed to be 5 cm and 9 cm/sec, respectively.<sup>7)</sup> The liquid holdup within the packed section is assumed to be ~ 10 % of the superficial volume of the section.<sup>8)</sup>

In the new cascade, the number of the columns is halved. The number of the output streams is just three. The DT stream produced by the TSTA cascade is not practically needed. The new cascade has ~ 1.5 times more tritium inventory owing to the large size of the second column.

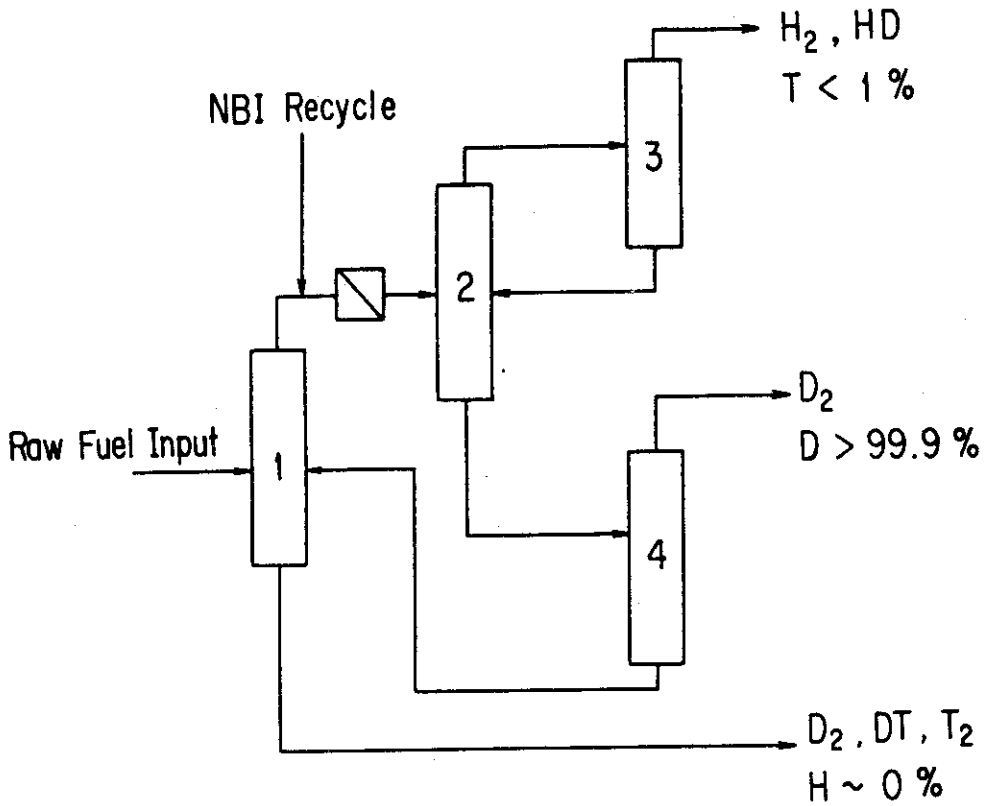


Fig. 5.1 Cryogenic distillation column cascade proposed at Argonne National Laboratory. This figure should be compared with Fig. 1.2.

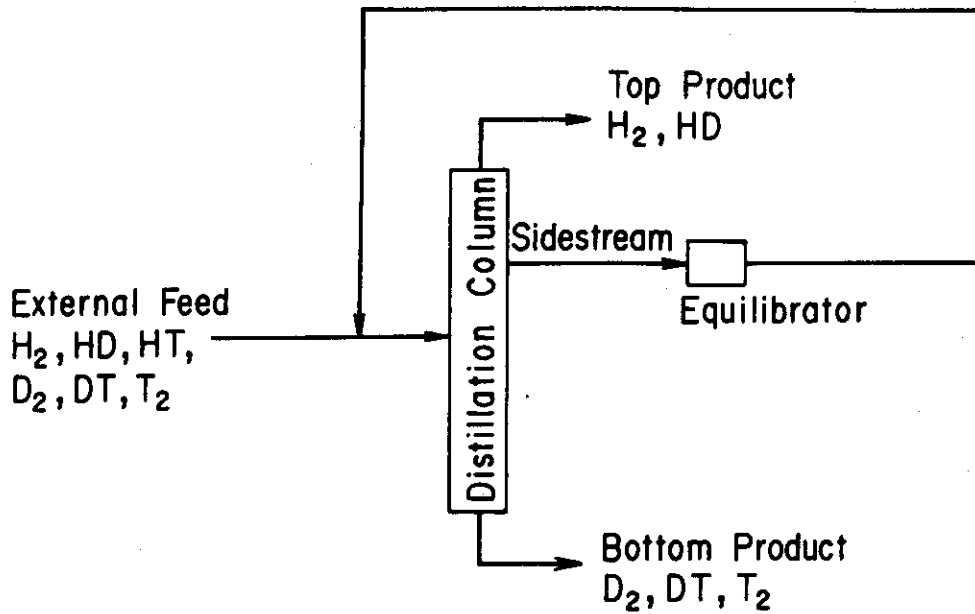


Fig. 5.2 Flow schematic of a column with a feedback stream processing all the six molecular species of hydrogen isotopes. The internal feed location is assumed to be identical with the external feed location. Protium and tritium are almost completely separated without any regard to deuterium. This figure should be compared with Fig. 3.1.

Number of Total Stages = 80  
 Feed Stage Number = 40  
 Sidestream Stage Number = 30

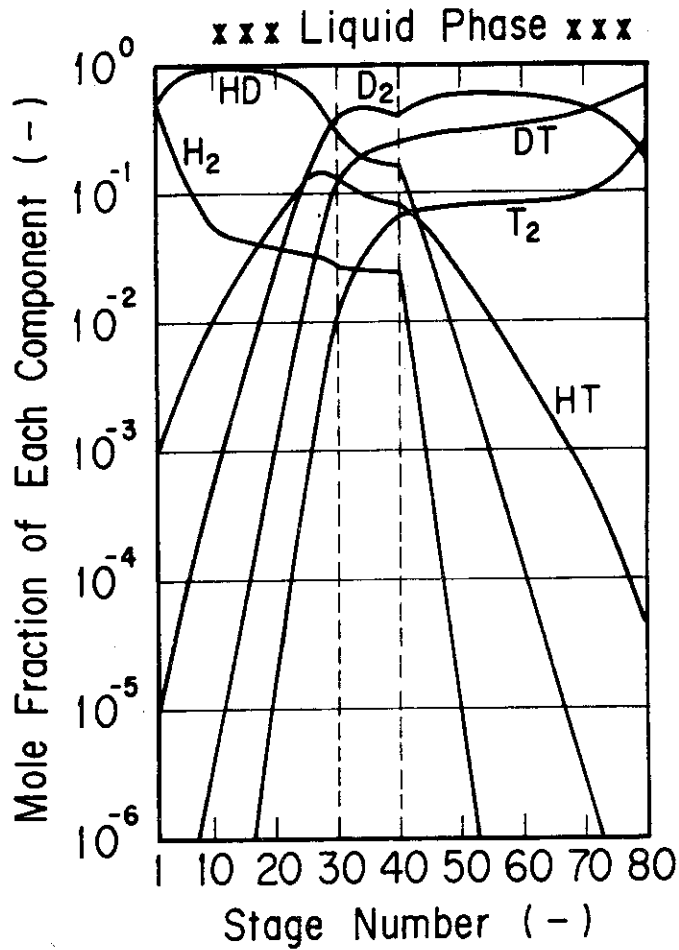


Fig. 5.3 Typical composition profile within the column shown in Fig. 5.2. As in Fig. 3.2, HT represents an interesting profile.

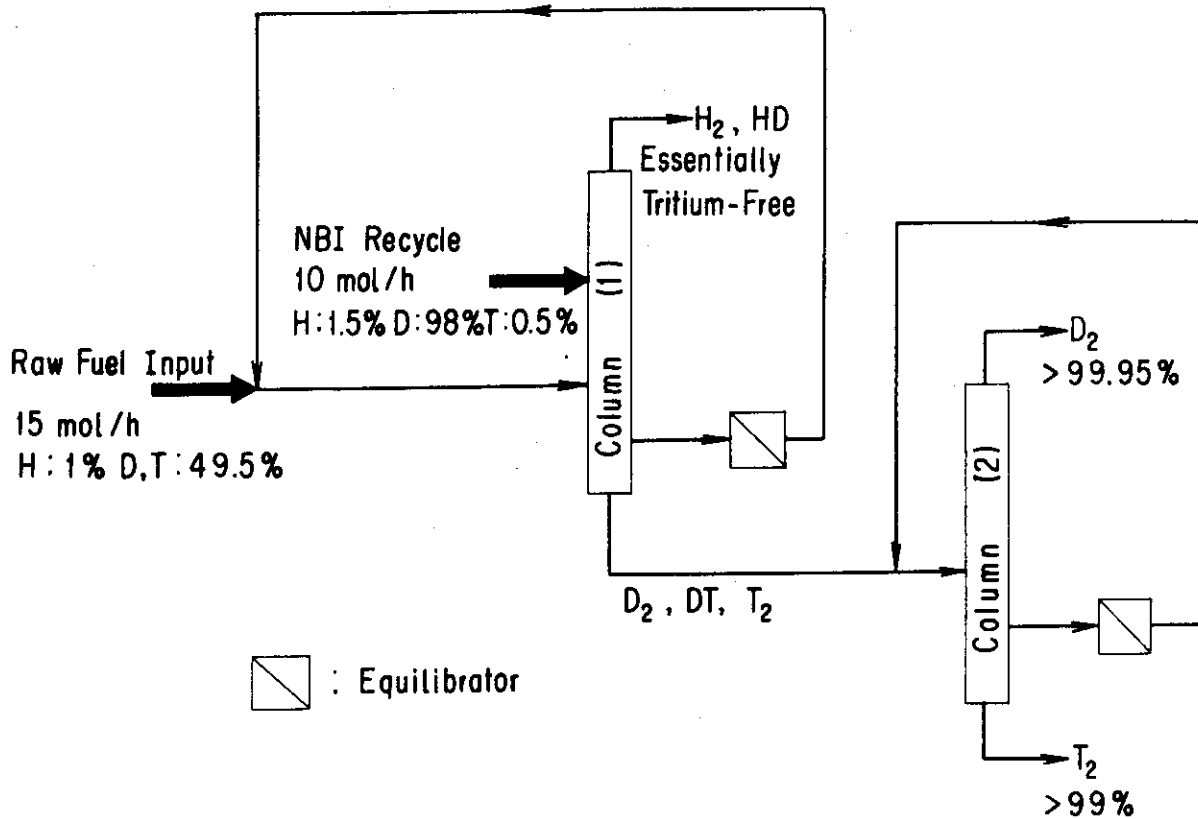


Fig. 5.4 New column cascade proposed as a possible alternative to the TSTA cascade shown in Fig. 1.2. The second column is a D-T separation column with a feedback stream which is similar to the column shown in Fig. 3.1. In the simulation of the second column, however, the feed is considered the six component system.

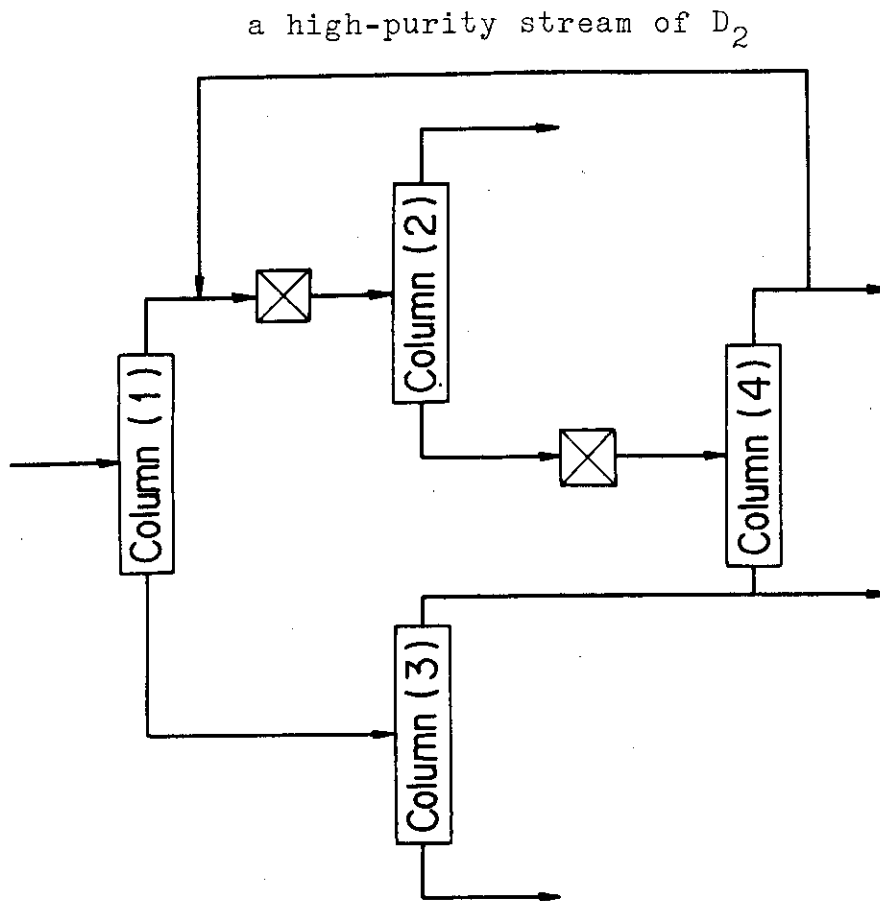


Fig. 5.5 Cascade configuration of the TSTA cascade in the case where the flow rate of the NBI recycle is too small. The NBI recycle is combined with the raw fuel input and the combined stream is fed to column(1). This figure should be compared with Fig. 1.2.

## 6. EFFECTS OF HELIUM ON CHARACTERISTICS OF HYDROGEN ISOTOPE DISTILLATION COLUMN

### 6.1 Steady state simulation

Although it is clear that such impurities as N, O, C and Ar must be removed from hydrogen isotopes before the isotope separation, some workers doubt that helium removal is imperative. It is a highly interesting subject to analyze helium effects on steady state and dynamic column behavior. The analysis has first been performed by the author<sup>1)</sup> choosing the TSTA cascade as an example (see Fig. 6.1). Based on design study for the presently-conceived tokamak type reactor, the helium percentage in the raw fuel input is expected to be in the range from 1 % to 10 %. All the helium goes to the top of column(2). It is obvious that column(2) is mainly affected by helium. In the simulation, the mixture is treated as a seven component system of He, H<sub>2</sub>, HD, HT, D<sub>2</sub>, DT and T<sub>2</sub>. The most significant physico-chemical parameter affecting the results of computer simulation is doubtlessly the volatility of helium. The calculational procedure of the volatility of helium is described in ref. 1.

The steady state simulation results are briefly summarized in Table 6.1. A higher percentage of helium in the raw fuel input requires a heavier condenser load and a higher column pressure. If it is 5 %, for instance, both the condenser load and column pressure are doubled. If it is 10 %, the packed height is also required to be increased by ~ 25 %, owing to considerable decreases in relative volatilities for the six

molecular species of hydrogen isotopes caused by the high column pressure. Thus, a higher column pressure, a lower inlet temperature and a larger flow rate of the refrigerant gas at the condenser, a larger heat transfer area at the condenser, and a larger inner diameter of the column must be considered in the design stage to accommodate helium. However, a significantly high percentage of helium exceeding 5 % in the raw fuel input may be unacceptable because the pressure required is considerably high.

## 6.2 Dynamic simulation

Since the flow rate of the top gas from column(2) is very small, the flow rate is manipulated essentially by an on-off mode. If an unacceptably high tritium level is observed in the top gas, its flow is shut off (actually, a flow of ~ 10 % of the full-normal flow is withdrawn for the gas analysis) until the specified low level is recovered. The author has studied helium effects on the on-off control operation for the tritium level.

Before describing the simulation results, the author wishes to emphasize the importance of vapor holdups in dynamic simulation.<sup>2)</sup> Table 6.2 gives the component material balances to be solved. As explained in the table, in cases of no helium  $\alpha$  is not far from unity for all the components, and  $\alpha H_{Vj}$  can be neglected compared with  $H_{Lj}$  ( $j = 2, \dots, N$ ) or  $(H_{Lj} + H_{Vj})$  can be

regarded as an 'overall' holdup ( $j = 1$  or  $j = 1, \dots, N$ ). On the other hand, the order of magnitude of  $\alpha$  of helium is  $10^2 - 10^3$ . Furthermore, its value varies greatly depending on the liquid composition and temperature. Hence, in cases where helium is present, the contribution of the terms including the vapor holdups is great, and  $dy_{i,j}/dt$  must be treated in a rigorous manner. The author<sup>1,2)</sup> has developed the working equations for such cases as given in Table 6.3. The calculation of  $\partial T_j / \partial x_{i,j}$  ( $i = 1, \dots, m-1$ ;  $j = 1, \dots, N$ ) and the matrix inversion at each iterative step are time consuming but unavoidable to draw qualitatively correct conclusions.

In cases of no helium, the tritium level control is quite successful as shown in Fig. 6.2. After the top gas is shut off, the tritium level at the top decreases steadily. During the operation, the condenser temperature drop is only  $\sim 0.01$  K. However, in the case of 5 % He in the raw fuel input, the condenser temperature decreases quite rapidly (from  $\sim 20.5$  K to  $\sim 16.5$  K in fifteen minutes) after the top flow is shut off (see Fig. 6.3). It should be noted that the dynamic simulation was performed by assuming that the column pressure and heat removal rate at the condenser are maintained constant during the operation, and then we obtained Fig. 6.3. In the actual operation, it will be extremely difficult for the condenser capacity to catch up with the heat addition rate at the reboiler, owing to the dramatical decrease in the temperature difference for heat transfer at the condenser. Thus, the liquid in the reboiler will vaporize and a significant pressure rise will occur. It will be impractical

to perform all the three control operations successfully : the tritium level control, pressure control and liquid level control for the reboiler. In the case of 1 % He in the raw fuel input, the condenser temperature drop is not so serious as shown in Fig. 6.4, and no big problem may be caused.

### 6.3 Concluding remarks

The effects of helium on dynamic column behavior are much larger than on steady state behavior. The conclusion is that if the helium percentage in the raw fuel input has a significant value ( $> 1\%$ ), helium must be removed before the isotope separation system. If the percentage is adequately low ( $< 1\%$ ), no special helium separator may be needed, but a larger condenser and a larger inner diameter of the column should be considered in the design stage.

Experimental study on the helium effects is strongly desired in the near future to verify the simulation results. The author now has two computer codes, CRYDIS-H1 and CRYDIS-H2, for analyzing the helium effects on steady state and dynamic column behavior, respectively. It should be noted that CRYDIS-N and CRYDIS-D are not applicable to such analyses because the simulation models to be used are considerably different.

## NOTATION

- $F_j$  = flow rate of feed stream supplied to j'th stage (mol/h)  
 $H_j$  = overall holdup on j'th stage (mol)  
 $H_{Lj}$  = liquid holdup on j'th stage (mol)  
 $H_{Vj}$  = vapor holdup on j'th stage (mol)  
 $K_{i,j}$  = vapor-liquid equilibrium ratio for i'th component  
on j'th stage (-)  
 $L_j$  = flow rate of liquid stream leaving j'th stage (mol/h)  
 $m$  = total number of components (-)  
 $N$  = number of total theoretical stages (-)  
 $T_j$  = temperature on j'th stage (K)  
 $t$  = time (h)  
 $U_j$  = flow rate of liquid sidestream from j'th stage (mol/h)  
 $V_j$  = flow rate of vapor stream leaving j'th stage (mol/h)  
 $W_j$  = flow rate of vapor sidestream from j'th stage (mol/h)  
 $x_{i,j}$  = mole fraction of i'th component in liquid stream  
leaving j'th stage (-)  
 $y_{i,j}$  = mole fraction of i'th component in vapor stream  
leaving j'th stage (-)  
 $z_{i,j}$  = mole fraction of i'th component in feed stream  
supplied to j'th stage (-)  
 $\alpha$  = average volatility (-)

REFERENCES

- 1) Kinoshita, M. : "Effects of Helium on Separation Characteristics of Cryogenic Distillation Column Cascade for Fusion Reactor," To be published in Fusion Technol.
- 2) Kinoshita, M. : "A Simple Model for Dynamic Simulation of Stage Separation Processes within which Very Volatile Components are Present," Submitted to AIChE J.
- 3) Kinoshita, M. : JAERI-M 82-214, Japan Atomic Energy Research Institute (1982).
- 4) Kinoshita, M. : "Studies on Simulation Procedures for Stage Processes in Fusion Fuel Cycle and Distillation Systems," Doctoral Dissertation, Kyoto University (1983).
- 5) Howard, G. M. : AIChE J., 16, 1022 (1970).

Table 6.1 Summary of helium effects on steady state specifications of column(2).

Helium percentage in raw fuel input	Condenser temperature	Condenser load	Operating pressure	Packed height
0 %	22.13 K	62 W	1 atm	3.9 m
1 %	20.85 K	80 W	1 atm	3.9 m
5 %	20.34 K	134 W	2 atm	3.9 m
10 %	20.66 K	178 W	4 atm	4.8 m

Note : The flow rate of tritium lost from the top of the column is almost unchanged in the four cases.

The column pressure is assumed so that the condenser temperature becomes about 20.5 K in cases where helium is present. More details are described in ref. 1.

Table 6.2 Component material balances for dynamic simulation.

$$\begin{aligned}
 & \underline{H_{L1}}(dx_{i,1}/dt) + H_{V1}(dy_{i,1}/dt) = V_2y_{i,2} - V_1y_{i,1} - L_1x_{i,1} \\
 & \underline{H_{Lj}}(dx_{i,j}/dt) + H_{Vj}(dy_{i,j}/dt) = L_{j-1}x_{i,j-1} + V_{j+1}y_{i,j+1} \\
 & \quad - (L_j + U_j)x_{i,j} - (V_j + W_j)y_{i,j} + F_jz_{i,j}, \\
 & \quad (j = 2, \dots, N-1) \\
 & \underline{H_{LN}}(dx_{i,N}/dt) + H_{VN}(dy_{i,N}/dt) = L_{N-1}x_{i,N-1} - L_Nx_{i,N} \\
 & \quad - V_Ny_{i,N} + F_Nz_{i,N}
 \end{aligned} \quad \left. \vphantom{\begin{aligned} & \underline{H_{L1}}(dx_{i,1}/dt) + H_{V1}(dy_{i,1}/dt) = V_2y_{i,2} - V_1y_{i,1} - L_1x_{i,1} \\ & \underline{H_{Lj}}(dx_{i,j}/dt) + H_{Vj}(dy_{i,j}/dt) = L_{j-1}x_{i,j-1} + V_{j+1}y_{i,j+1} \\ & \quad - (L_j + U_j)x_{i,j} - (V_j + W_j)y_{i,j} + F_jz_{i,j}, \\ & \quad (j = 2, \dots, N-1) \\ & \underline{H_{LN}}(dx_{i,N}/dt) + H_{VN}(dy_{i,N}/dt) = L_{N-1}x_{i,N-1} - L_Nx_{i,N} \\ & \quad - V_Ny_{i,N} + F_Nz_{i,N} \end{aligned}} \right\} (6.1)$$

$$\begin{aligned}
 y_{i,j} = \alpha x_{i,j} & : \frac{(H_{Lj} + \alpha H_{Vj})(dx_{i,j}/dt)}{\sim H_j(dx_{i,j}/dt),} \\
 & H_j = H_{Lj} + H_{Vj}.
 \end{aligned}$$

Note : The term underlined in Eq.(6.1) is expressed by  $(H_{Lj} + \alpha H_{Vj}) \cdot (dx_{i,j}/dt)$  ( $j = 1, \dots, N$ ) if  $\alpha$  is considered constant. The decision on whether  $H_{Vj}$  is negligible or not must be made by comparing  $\alpha H_{Vj}$  with  $H_{Lj}$ . In cases of very large  $\alpha$ , the vapor holdup can be highly significant even if  $H_{Vj}$  is much smaller than  $H_{Lj}$ .<sup>2)</sup>

Table 6.3 Working equations for dynamic simulation  
incorporating vapor holdups.

$$\begin{bmatrix} dx_{1,j}/dt \\ \vdots \\ dx_{m,j}/dt \end{bmatrix} = \begin{bmatrix} A_{11,j} & \dots & A_{1m,j} \\ \vdots & \ddots & \vdots \\ A_{m1,j} & \dots & A_{mm,j} \end{bmatrix}^{-1} \begin{bmatrix} D_{1,j} \\ \vdots \\ D_{m,j} \end{bmatrix}, \quad (j = 1, \dots, N), \quad (6.2)$$

where

$$A_{kk,j} = H_{Lj} + K_{k,j}H_{Vj} + x_{k,j}H_{Vj}g_{k,k,j}, \quad (k = 1, \dots, m-1),$$

$$A_{kn,j} = x_{k,j}H_{Vj}g_{k,n,j}, \quad (n = 1, \dots, m-1; k = 1, \dots, m-1; \\ n \neq k),$$

$$A_{km,j} = 0, \quad (k = 1, \dots, m-1),$$

$$A_{mk,j} = x_{m,j}H_{Vj}g_{m,k,j}, \quad (k = 1, \dots, m-1),$$

$$A_{mm,j} = H_{Lj} + K_{m,j}H_{Vj},$$

and

$$g_{i,k,j} = \partial K_{i,j} / \partial x_{k,j} + (\partial K_{i,j} / \partial T_j)(\partial T_j / \partial x_{k,j}).$$

Note : The terms,  $D_{i,j}$ 's, denote the right sides of Eq.(6.1).

The term,  $\partial T_j / \partial x_{i,j}$ , is calculated from the requirement that the sum of the vapor mole fractions be unity.<sup>3-5)</sup>

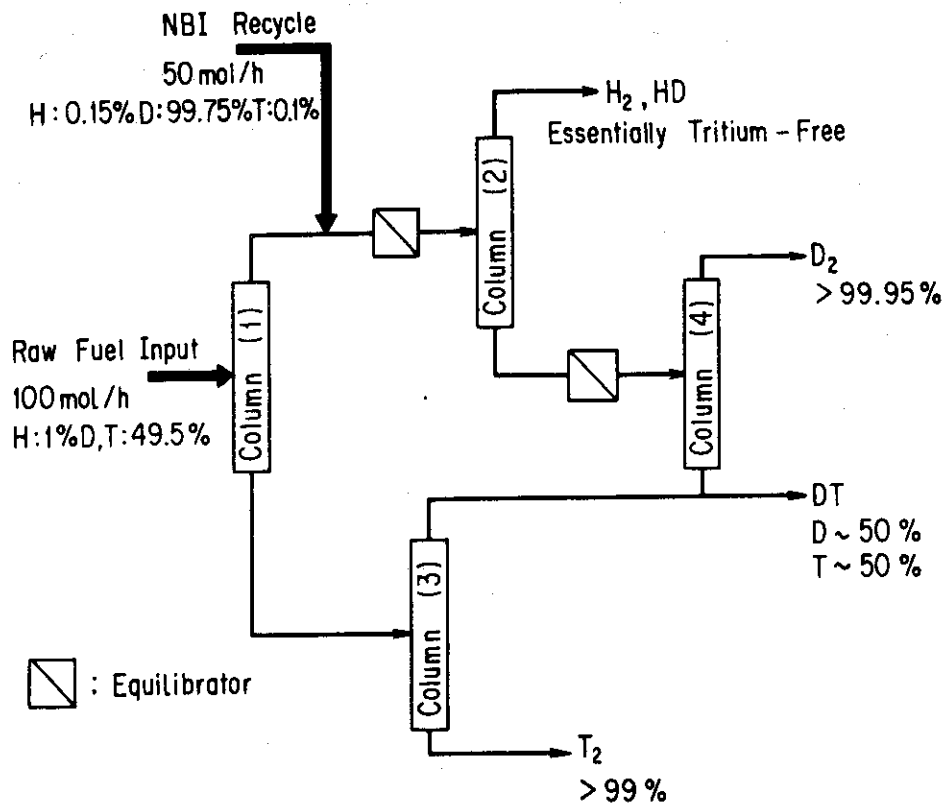


Fig. 6.1 Column cascade chosen for the analysis of the helium effects. The configuration is identical with that of the TSTA cascade shown in Fig. 1.2. The composition of the NBI recycle given here is based on the actual TSTA operation scheduled in Los Alamos.

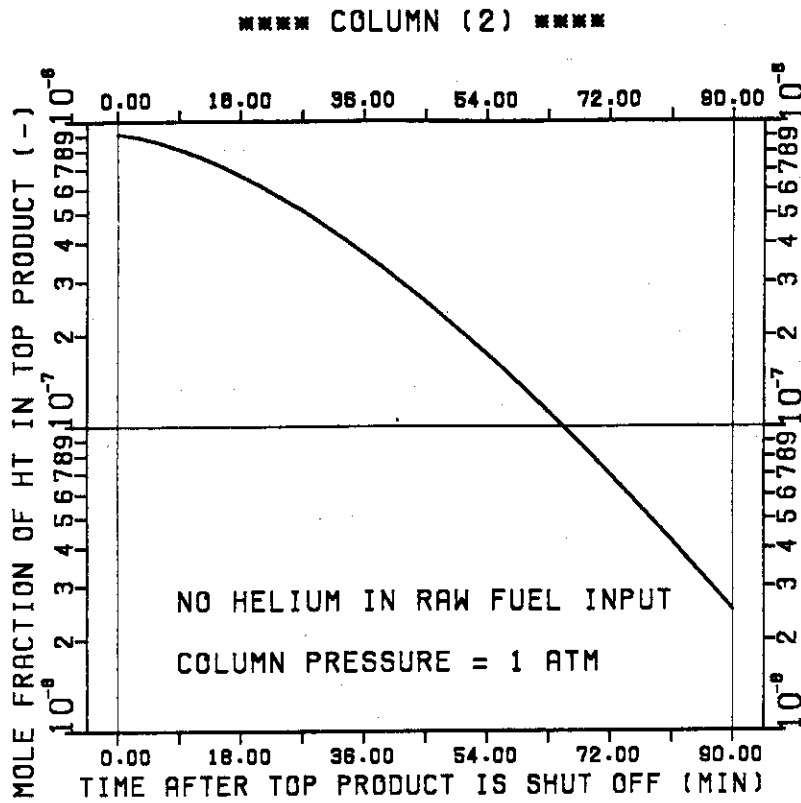


Fig. 6.2 Variation of the mole fraction of HT in the top gas after the top flow is almost shut off. An example is given here. Helium is not present within the column. A flow of 10 % of the full-normal flow is assumed to be withdrawn for the gas analysis.

\*\*\*\*\* COLUMN (2) \*\*\*\*\*

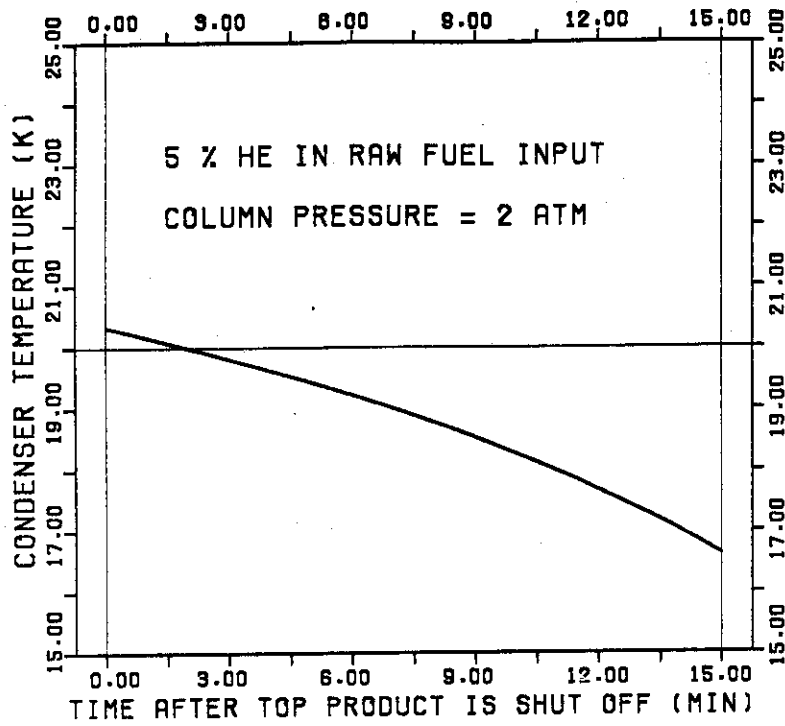


Fig. 6.3 Remarkable temperature drop at the condenser observed after the top flow is almost shut off. An example is given here in the case of 5 % He in the raw fuel input. Details on the calculational conditions are described in ref. 1.

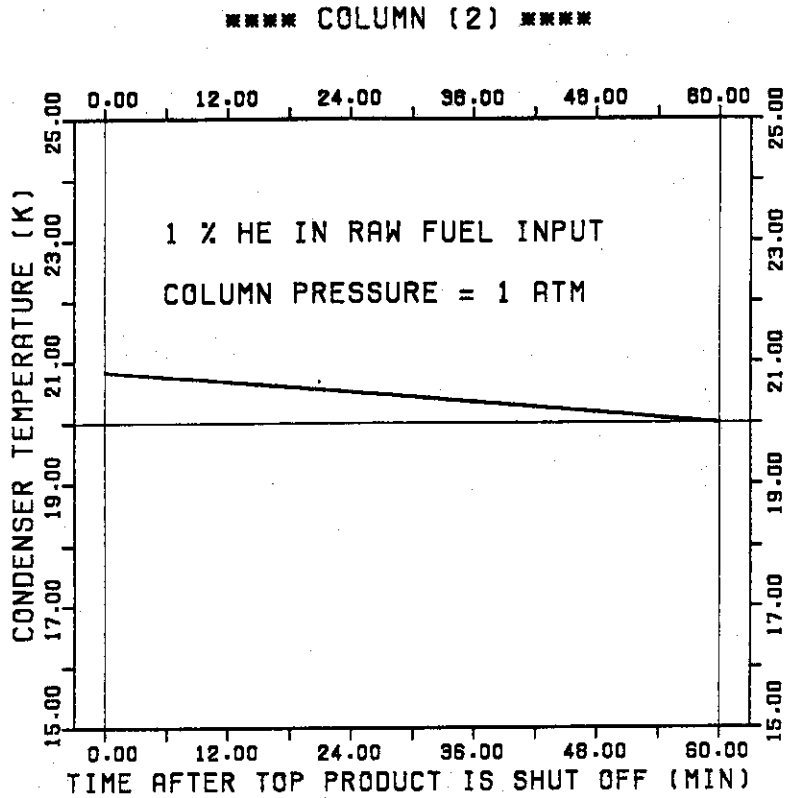


Fig. 6.4 Temperature drop at the condenser observed in the case of 1 % He in the raw fuel input after the top flow is almost shut off. This figure should be compared with Fig. 6.3.

## 7. START-UP ANALYSIS FOR COLUMN CASCADE

### 7.1 Significance of a start-up analysis for a cascade composed of multiple columns

In the previous chapters, a variety of computer simulation studies or numerical analyses were performed, but there still is a very significant category left with which no workers have dealt yet. It is a start-up analysis. When the operation of a column cascade is started, there is essentially no composition profile within any of the columns, and the cascade presents no separation performance. One of the most serious concerns is to write a start-up scenario for the cascade indicating how the full-normal performance is successfully attained.

The author<sup>1)</sup> has performed a start-up analysis choosing the TSTA cascade shown in Fig. 1.2 as an example. Four scenarios were considered and analyzed, and the last two were proposed as successful scenarios. A significant amount of information useful to a start-up of any cascade was obtained. Here is a brief summary of the results.

### 7.2 Scenarios 1 and 2

In scenario 1, a gas mixture having the average composition of the two input streams (raw fuel input and NBI recycle) is prepared and charged into the four columns which have adequately been refrigerated. Then, the four columns are put into the total

reflux operation simultaneously. Steady state is reached in ~ 1.5 h, but the composition profiles thus obtained do not meet the output specifications required yet. Hence, the four output streams cannot be withdrawn as products, and the operation must be switched to the total recycle mode shown in Fig. 7.1. However, it is obvious that the total recycle operation does not present the full-normal condition, because the inventories of H, D and T within the cascade in this stage are far from those in the full-normal condition.

The inventories of H, D and T within the columns in the full-normal condition have been calculated by the author and the results are given in Table 7.1. In scenario 2, the composition of the gas mixture to be charged into the columns is determined so that the inventories of the three elements within the cascade are equal to those in the full-normal condition. However, the computer simulation predicted that even the use of scenario 2 would not achieve the condition under which the requirements for the output streams were met.

### 7.3 Scenario 3

In scenario 3, four different gas mixtures to be charged are prepared as per Table 7.1. For example, column(1) has 0.57 % H, 76.73 % D and 22.69 % T in the full-normal condition. Hence, a gas mixture having this composition is charged into column(1). However, T is not charged into column(2) and H is

not charged into columns(3) and (4) as illustrated in Fig. 7.2. After the charge of the gas mixtures is completed, the four columns are put into the total reflux operation. Steady state is reached in ~ 2 h. Then, the tritium level at the top of column(2) is zero, the deuterium purity at the top of column(4) is almost 100 %, and the tritium purity at the bottom of column(3) exceeds 99 % : the output streams can be withdrawn as products (see Fig. 7.3). The computer simulation predicted that the steady state of the full-normal condition would be achieved in ~ 6 h and the specifications of the output streams would be kept quite satisfactory until this achievement. As an example, the variation of the tritium level in the top gas from column(2) after the operation is switched to the full-normal mode is shown in Fig. 7.4.

#### 7.4 Scenario 4

In scenario 4, the gas mixture prepared in scenario 2 is charged into column(1), and column(1) alone is operated at the total reflux mode (step 1 ; Fig. 7.5(a)). After the steady state is reached, columns(2) and (3) are fed from the top and bottom of column(1), respectively (step 2 ; Fig. 7.5(b)). The three columns are operated at the total reflux mode (step 3 ; Fig. 7.5(c)). While column(3) is still operated at the total reflux mode, column(4) is fed from the bottom of column(2) (step 4 ; Fig. 7.6(a)). The four columns are operated at the

total reflux mode (step 5 ; Fig. 7.6(b)). The computer simulation predicted that the composition profiles achieved in step 5 would not meet the output specifications required, so the operation is switched to the total recycle mode (step 6 ; Fig. 7.1). The purities of the tritium and deuterium streams reach the desired values in several hours. The tritium level in the top gas from column(2) decreases rather rapidly in the initial period as shown in Fig. 7.7, but the decreasing rate is greatly decelerated in several hours. The tritium level after 10 h is approximately three times higher than the full-normal value. The level remains essentially constant even if the total recycle operation is further continued. Hence, the operation must be switched to another mode. First, the author assumed that the full-normal mode was started on condition that the top flow from column(2) was shut off until the tritium level decreased to the full-normal level. However, according to the computer prediction, the purity of the deuterium stream from the top of column(4) was greatly deteriorated if the above-mentioned operation method was chosen : while the top flow was shut off, the flow rate of protium fed to column(4) continued to increase, with the result that the deuterium purity was largely deteriorated because all the protium fed to column(4) was recovered at the top. Next, the author assumed that the full-normal mode was started by opening the top flow from column(2). As shown in Fig. 7.8, the tritium level in the top gas decreases to the full-normal level rather rapidly, so the assumed operation method seems acceptable. Then, the steady state is reached in several hours.

## 7.5 Concluding remarks

The two scenarios which are expected to present successful start-up are compared in Table 7.2. Both have advantages and disadvantages. In any case, the compositions of the gas mixtures to be charged into the columns must carefully be prepared, because they remarkably affect the start-up characteristics. To determine the compositions, the inventories of H, D and T within each column under the full-normal condition must be calculated as accurately as possible. The tritium level control for the column(2) top gas conflicts with the purity control for the deuterium stream from column(4). To start the full-normal operation mode, the tritium level in the column(2) top gas needs to be adequately low, and the purity of the deuterium stream is required to be almost 100 %.

A set of computer codes, TSTA-ISS-SA, are available to perform the start-up analysis for the TSTA cascade. The author is now developing another set of computer codes for the start-up analysis for the new cascade proposed in chapter 5.

## REFERENCES

- 1) Kinoshita, M., J. R. Bartlit, and R. H. Sherman : "A Start-Up Analysis of Four Interlinked Distillation Columns for Hydrogen Isotope Separation," Submitted to Fusion Technol.

Table 7.1 Inventories of H, D and T in full-normal condition.

Column	H (g-atom)	D (g-atom)	T (g-atom)
(1)	0.1175	15.73	4.652
(2)	3.981	10.04	0.4451E-1
(3)	0.1063E-5	3.689	11.53
(4)	0.2642E-2	36.38	3.820
Total <sup>*)</sup>	4.101 (4.56%)	65.84 (73.16%)	20.05 (22.28%)

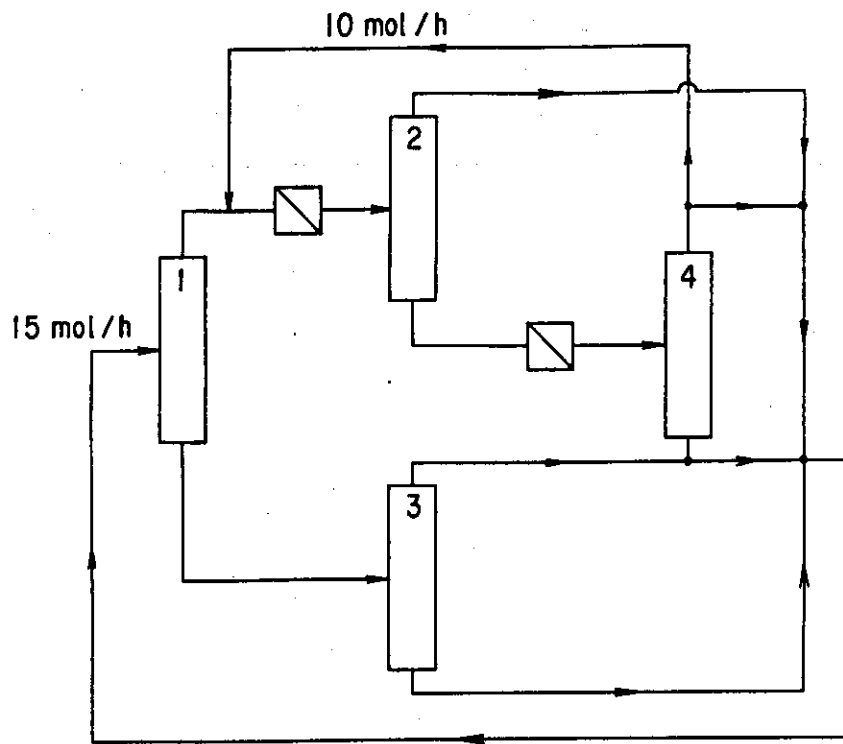
\*) In scenario 2, a gas mixture (equilibrated at 298 K) having these atomic percentages is charged into the four columns.

The four columns are operated at the total reflux mode and then the total recycle mode.

Table 7.2 Comparison between scenarios 3 and 4.

Scenario	Advantages	Disadvantages
3	<ul style="list-style-type: none"> <li>• Composed of only two operation modes.</li> <li>• Comparatively short time consumed.</li> </ul>	<ul style="list-style-type: none"> <li>• Preparation of four gas mixtures of different compositions.</li> </ul>
4	<ul style="list-style-type: none"> <li>• Free from complexity of charging four separate compositions.</li> </ul>	<ul style="list-style-type: none"> <li>• Composed of seven operation modes.</li> <li>• Significantly longer time consumed.</li> </ul>

Note : The total start-up time consumed is ~ 10 h in scenario 3 and ~ 23 h in scenario 4.



TOTAL RECYCLE OPERATION

Fig. 7.1 Total recycle operation mode. This mode is used after the total reflux operation of the four columns and in cases where the product streams do not satisfy the specifications required.

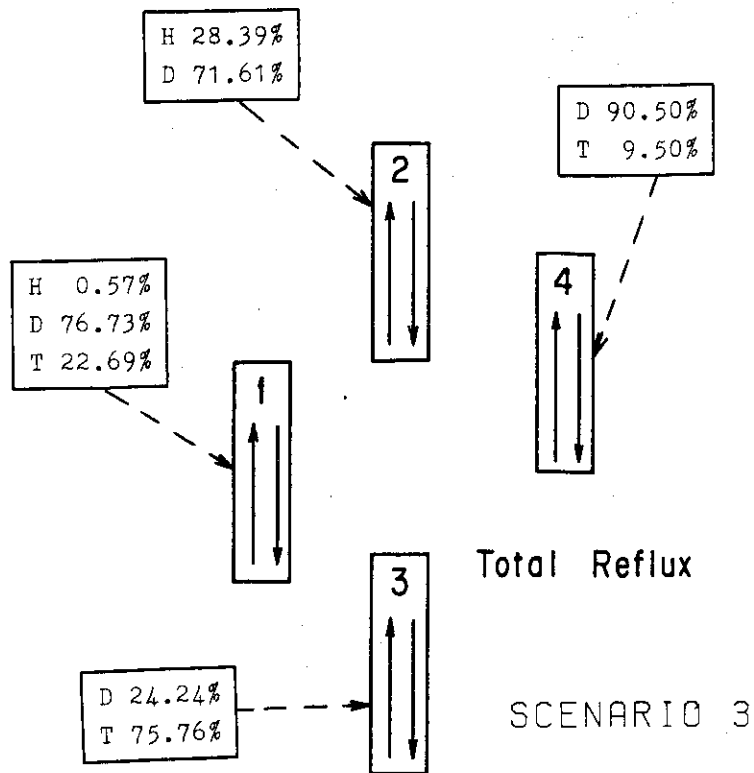


Fig. 7.2 Compositions of the four gas mixtures charged into the four columns, respectively. After the charge is completed, the four columns are put into the total reflux operation simultaneously.

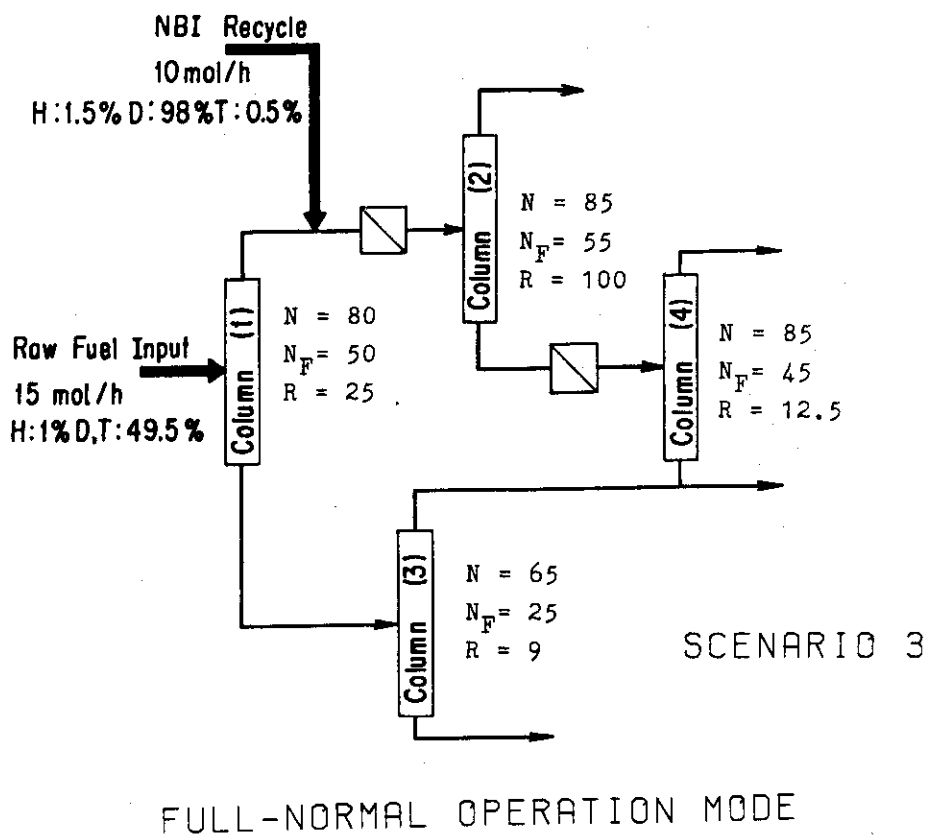


Fig. 7.3 Full-normal operation mode. This mode is used after the total reflux operation of the four columns or the total recycle operation and in cases where the output specifications required are almost met.

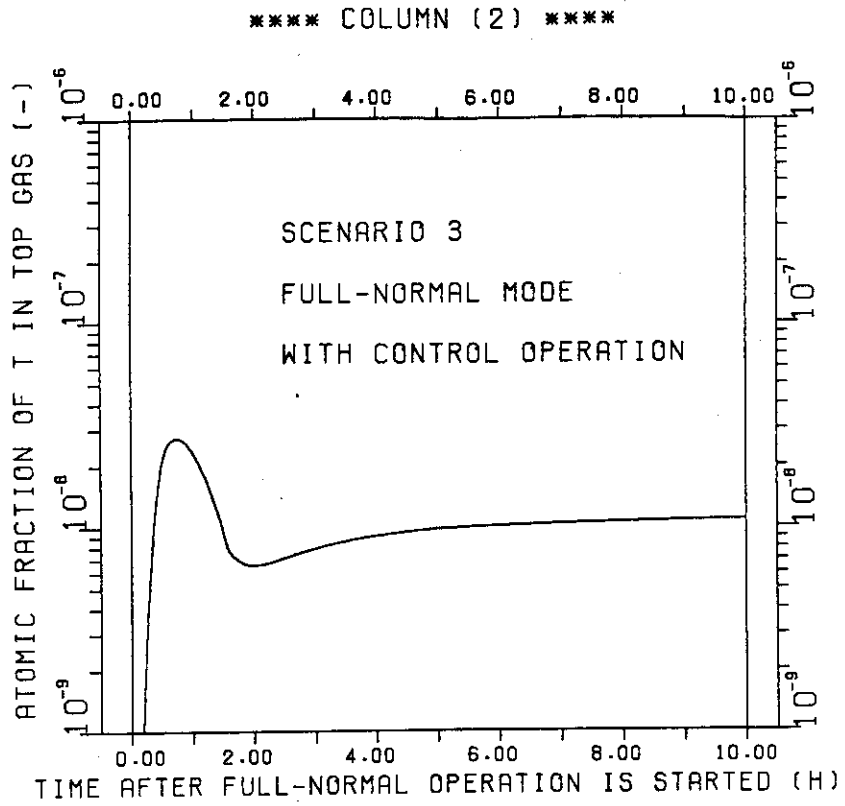


Fig. 7.4 Variation of the tritium level in the top gas from column(2) after the full-normal operation mode is started in scenario 3.<sup>1)</sup>

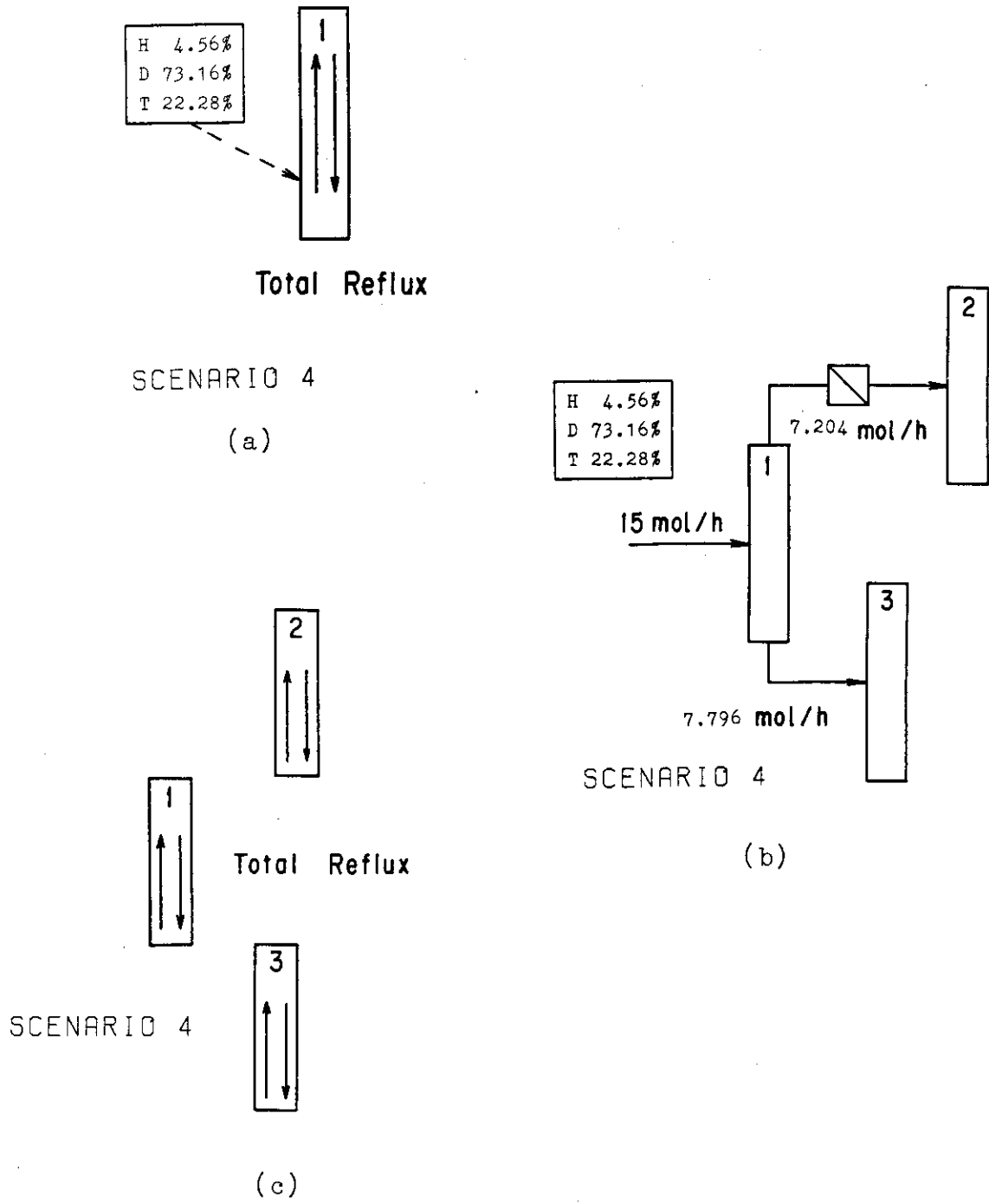
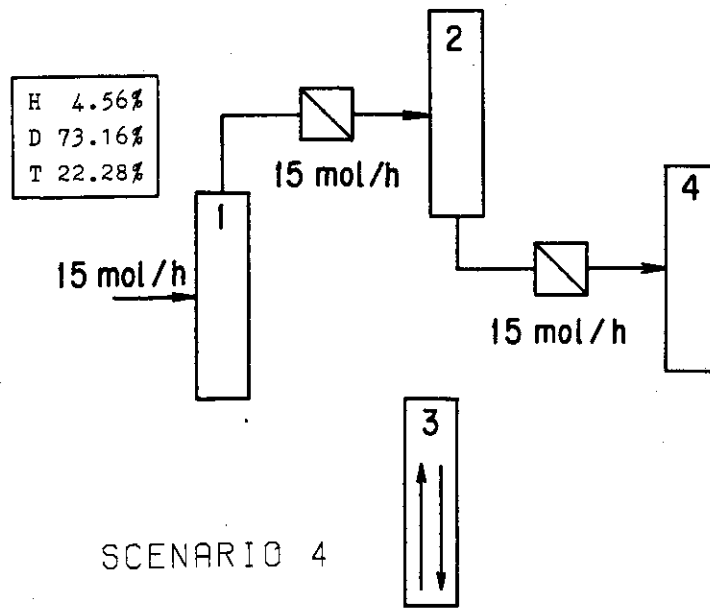
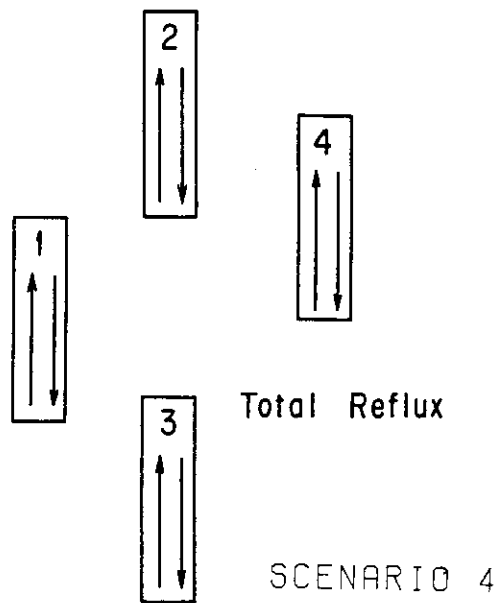


Fig. 7.5 (a) Step 1 in scenario 4.  
 (b) Step 2 in scenario 4.  
 (c) Step 3 in scenario 4.



(a)



(b)

Fig. 7.6 (a) Step 4 in scenario 4.

(b) Step 5 in scenario 4.

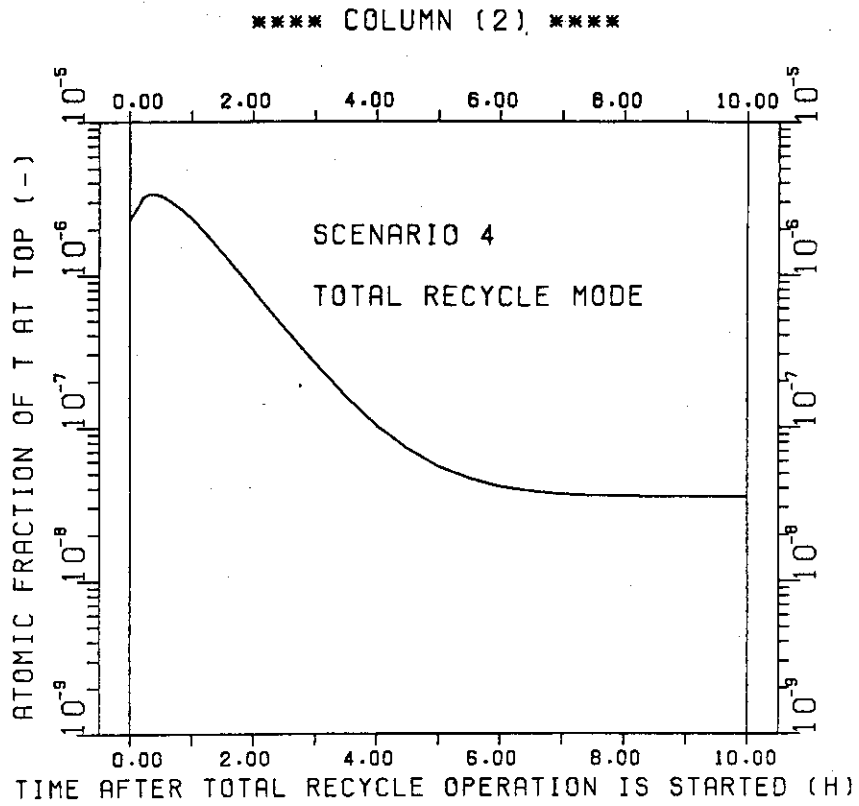


Fig. 7.7 Variation of the tritium level in the top gas from column(2) after the total recycle operation mode (step 6) is started in scenario 4.

\*\*\*\* COLUMN (2) \*\*\*\*

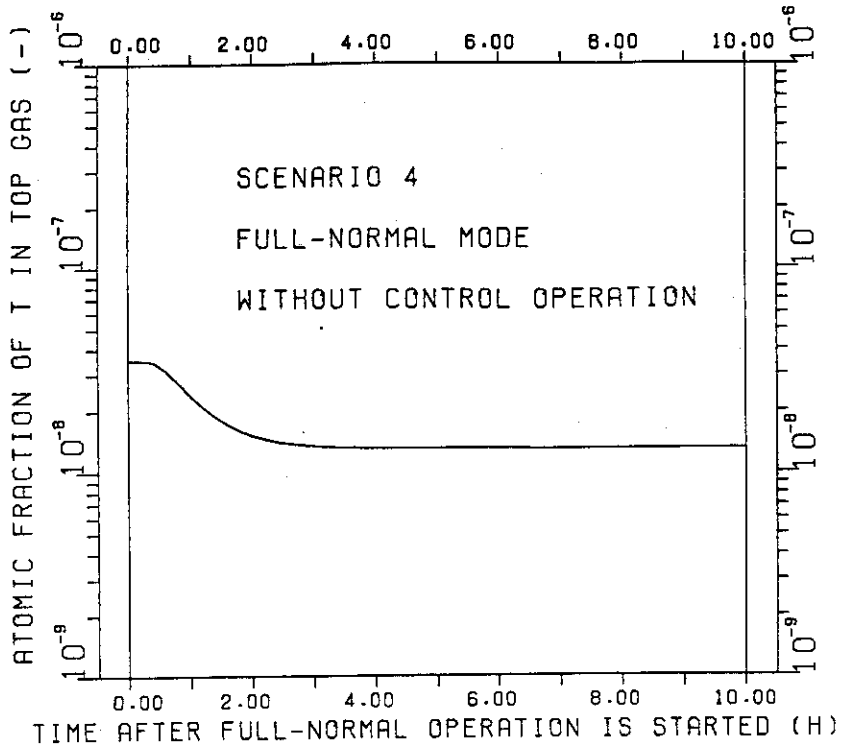


Fig. 7.8 Variation of the tritium level in the top gas from column(2) after the full-normal operation mode (step 7) is started in scenario 4.

## 8. PRELIMINARY EXPERIMENTAL STUDY

### 8.1 Significance of HETP and purpose of the experiment

In the previous chapters, the behavior of the model column was studied in detail on a digital computer. The model column has separate stages, but the actual column is a packed column. Hence, to extend the simulation results for the model column to the actual column behavior, information on a key parameter HETP is absolutely needed. This essential parameter is usually determined so that the computer simulation for steady state compositions at the top and bottom gives the best fit to the experimental observation. It should be noted, however, that a value of HETP is obtained no matter how a simple model neglecting many factors is used in the simulation. In such cases, the measured value will vary to some extent depending on the experimental condition and becoming a function of the neglected factors. For instance, let us assume that the simulation model neglects decay heat of tritium. When the experiment is performed under a high tritium concentration condition, the measured value of HETP will be significantly larger than that under a low tritium concentration condition. Then, let us assume that the model is too conservative using unnecessarily low relative volatilities for components. The measured value of HETP will be excessively small. A problem caused is that in such example cases the HETP value varies greatly from condition to condition, and HETP loses its significance and is not a useful parameter any longer. The author believes that all the reported values of HETP for

the mixtures whose vapor-liquid equilibrium data are unknown or quite uncertain are not reliable at all.

To eliminate the above-mentioned problems, as many factors as possible should be accounted for in the simulation model. The number of the factors to be accounted for may be infinite, but the factors having trivial effects on the simulation results need not be considered. The author incorporated most of the significant factors in the model, but there was one essential factor neglected : it is the so-called hydraulic effect. A column has a large partial condenser and a wire holding the packings. The inner diameter of the condenser is far larger than that of the packed section. Hence, it may not be easy for the liquid falling from the condenser to the packed section to wet the packings near the top sufficiently. This is particularly true in cases of a rather small liquid flow rate (or equivalently, small vapor velocity within the column), and a significant decrease in the vapor/liquid interface area may occur near the top. The flow pattern of the liquid near the bottom of the packed section is greatly affected by the specifications of the wire,<sup>1)</sup> and it may be subject to the vapor velocity. Thus, the HETP value may depend on the vapor velocity. In addition, the vapor/liquid interface area may be dependent on the specifications of the packings. Hence, an essential subject is to study how the HETP value is affected by the factors which are not accounted for in the stage model, such as the vapor velocity, species and sizes of the packings. This subject can be studied by using a column separating  $N_2$  and Ar. The vapor-liquid equilibrium for this

mixture<sup>2)</sup> has extensively been studied and reliable data are available. A feature of columns in tritium systems for the fusion reactor is the relatively small inner diameter (1 - 10 cm) of the packed section. Therefore, the study was performed by using a column with a small inner diameter (~ 2 cm).

## 8.2 Experimental procedure and the simulation model used

A simplified diagram of the experimental apparatus is shown in Fig. 8.1. Liquid nitrogen is used as the refrigerant at the condenser. The wire holding the packings is conically shaped and has a large mesh.<sup>1)</sup> The inner diameter of the packed section is 1.94 cm. First, nitrogen gas is charged into the column. The gas is condensed at the condenser, and liquid thus formed falls to the packings. The liquid is then vaporized, thus removing heat corresponding to latent heat of vaporization of nitrogen. This phenomenon occurs repeatedly until the packed section is adequately refrigerated. After the refrigeration of the packed section during which nitrogen gas is charged several more times is completed, the refrigeration of the reboiler proceeds in a similar manner. Until the reboiler refrigeration is completed, a large amount of liquid is held within the packed section, thus the so-called pre-flooding is performed before the experiment. After the refrigeration of the whole column, the column is evacuated, and then a mixture of  $N_2$  and Ar is charged into the column. After the liquid level in the reboiler

reaches constant, the electric heater at the bottom is put on and distillation is started at the total reflux mode. The variation of the argon concentration in the vapor phase is measured by the gas chromatograph for the top, middle and bottom of the column.

The simulation model incorporates the nonideality of the  $N_2$ -Ar system and the large amount of vapor holdup in the condenser.<sup>1,3)</sup> A set of ordinary differential equations are solved by the Improved Euler method. The number of total theoretical stages is determined so that the calculated result for argon concentration for the top and bottom gives the best fit to the experimental observation. The calculational procedure for argon concentration at the middle is illustrated in Fig. 8.2.

### 8.3 Effect of the vapor velocity on HETP

First, Dixon Ring whose size was  $\sim 1/6$  of the inner diameter was chosen and the effect of the vapor velocity on HETP was studied. An example comparison between the computer calculation and experimental observation is shown in Fig. 8.3. All the three calculated lines are in very close agreement with the measured points. A significant result is that the agreement is also very good for the middle. This means that the middle point of the model column can be considered the middle point of the actual column. Thanks to this advantage, the stage model is a powerful tool, because the locations of feeds and sidestreams

can readily be determined for the actual column by referring to the simulation result.

Figure 8.4 shows the HETP value is  $\sim 5.5$  cm and almost independent of the vapor velocity. This result is consistent with the reported results by Sherman et al.<sup>4)</sup> for hydrogen isotope distillation and by Yamamoto and Kanagawa<sup>5)</sup> for water distillation. A feature common in these works is the small inner diameter of the column. Under our experimental condition, HETP can be expressed by

$$\text{HETP} = Z/(N - 2), \quad V(y_{\text{bot}} - y_{\text{top}}) = \int_0^Z r(V, z) dz, \quad (8.1)$$

where  $r$  is overall mass transfer rate of argon from vapor phase to liquid phase and can be regarded as the product of a term corresponding to the overall mass transfer coefficient and a term corresponding to the vapor/liquid interface area. The experimental results indicate that if  $V$  is halved, the total transfer rate of argon,  $V(y_{\text{bot}} - y_{\text{top}})$ , is also almost halved. Then, the term corresponding to the overall mass transfer coefficient decreases, but is still considerably larger than the half of the previous value ( note that this term is proportional to  $V^\alpha$  ;  $0 < \alpha < 1$  ). Hence, the term corresponding to the vapor/liquid interface area decreases also, and as a result the term,  $\int_0^Z r(V, z) dz$ , is also halved.

It should be noted that if the vapor velocity is too small, the agreement between the calculated line and experimentally measured points for the middle is not very good any longer

as shown in Fig. 8.5. In cases where the vapor velocity is very small, the flow rate of liquid falling from the condenser to the packings is also very small. In such cases, the liquid falls along the condenser wall rather slowly and is not capable of wetting the packings near the top sufficiently. Thus, the vapor/liquid interface area in the upper half of the column decreases significantly, and the above-mentioned discrepancy is observed for the middle.<sup>6)</sup>

#### 8.4 Comparison among the experimental results for Dixon Ring, Heli-pak, Helix and Coil Pack

The three packings, Heli-pak, Helix and Coil Pack were also tested. We should choose the packing species which gives the lowest value of HETP, the lowest pressure drop (or equivalently, the highest flooding velocity), and the best agreement on argon concentration between the calculation and experimental observation for the middle. Among the four species, Dixon Ring gave the best set of results.<sup>6)</sup> Dixon Ring has an exceptionally large void fraction, nevertheless its interface area is fairly large. The results may be ascribed to this feature. Packings having small void fractions and densely coiled structure like Coil Pack give an adequately low value of HETP, but are unfavorable in the other respects.

## 8.5 Concluding remarks

Unless the vapor flow rate within the column is excessively small, the stage model is a powerful tool in simulating actual column. The author is now investigating how the column performance is affected by the inner diameter of the column and the size of the packings.

After the preliminary experimental study with  $N_2$  and Ar, a hydrogen isotope distillation column will be constructed and studied.

## NOTATION

- $N$  = number of total theoretical stages (-)  
 $V$  = vapor flow rate (mol/h)  
 $y_{\text{bot}}$  = mole fraction of argon in vapor phase at the bottom of packed section (-)  
 $y_{\text{top}}$  = mole fraction of argon in vapor phase at the top of packed section (-)  
 $Z$  = height of packed section (cm)

## 8.5 Concluding remarks

Unless the vapor flow rate within the column is excessively small, the stage model is a powerful tool in simulating actual column. The author is now investigating how the column performance is affected by the inner diameter of the column and the size of the packings.

After the preliminary experimental study with  $N_2$  and Ar, a hydrogen isotope distillation column will be constructed and studied.

## NOTATION

- $N$  = number of total theoretical stages (-)  
 $V$  = vapor flow rate (mol/h)  
 $y_{\text{bot}}$  = mole fraction of argon in vapor phase at the bottom of packed section (-)  
 $y_{\text{top}}$  = mole fraction of argon in vapor phase at the top of packed section (-)  
 $Z$  = height of packed section (cm)

## REFERENCES

- 1) Yamanishi, T. and M. Kinoshita : J. Nucl. Sci. Technol.,  
21, 61 (1984).
- 2) Latimer, R. E. : AIChE J., 3, 75 (1957).
- 3) Kinoshita, M. : JAERI-M 82-214, Japan Atomic Energy Research  
Institute (1982).
- 4) Bartlit, J. R., W. H. Denton, and R. H. Sherman : Proc.  
3rd Topical Mtg. on Technol. of Controlled Nucl. Fusion,  
Santa Fe, NM, May 9-11, 1978, pp.778-783.
- 5) Yamamoto, I. and A. Kanagawa : J. Nucl. Sci. Technol.,  
16, 147 (1979).
- 6) Yamanishi, T. and M. Kinoshita : "Preliminary Experimental  
Study for Cryogenic Distillation Column with Small Inner  
Diameter, (II)," To be published in J. Nucl. Sci. Technol.

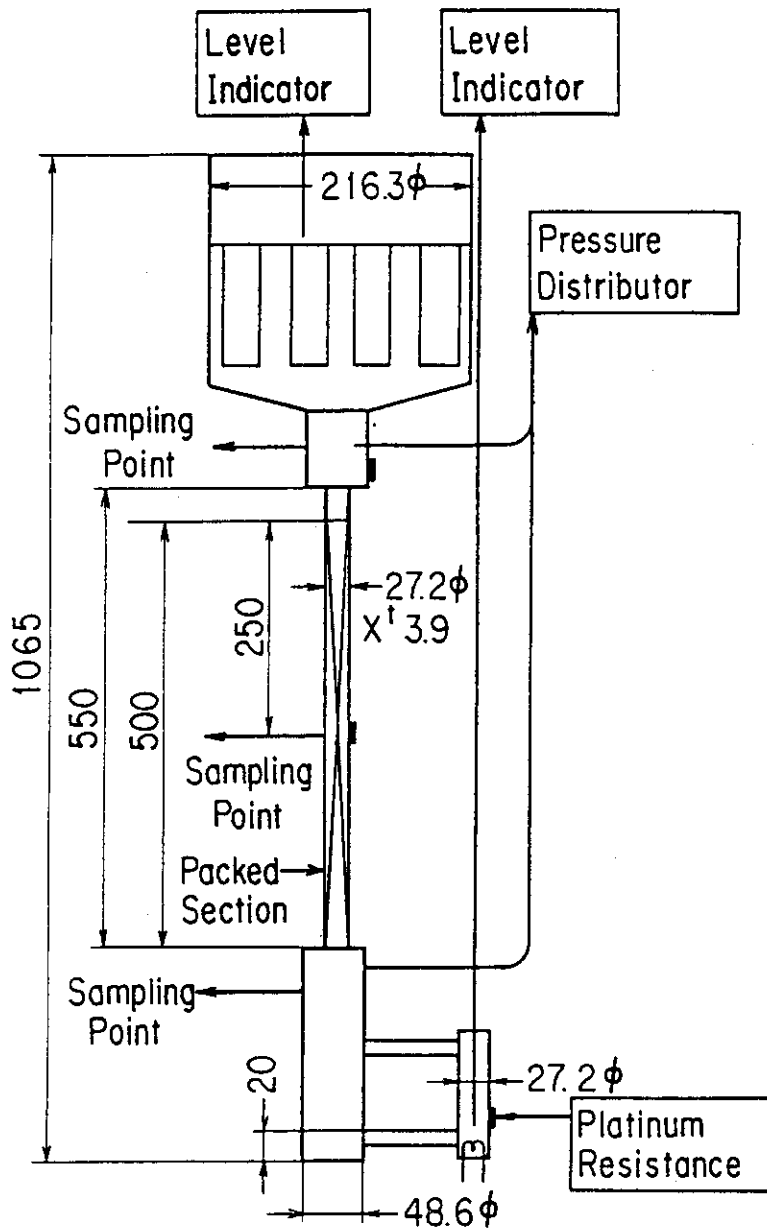


Fig. 8.1 Simplified diagram of the experimental apparatus.  
The height of the packed section is 50 cm.

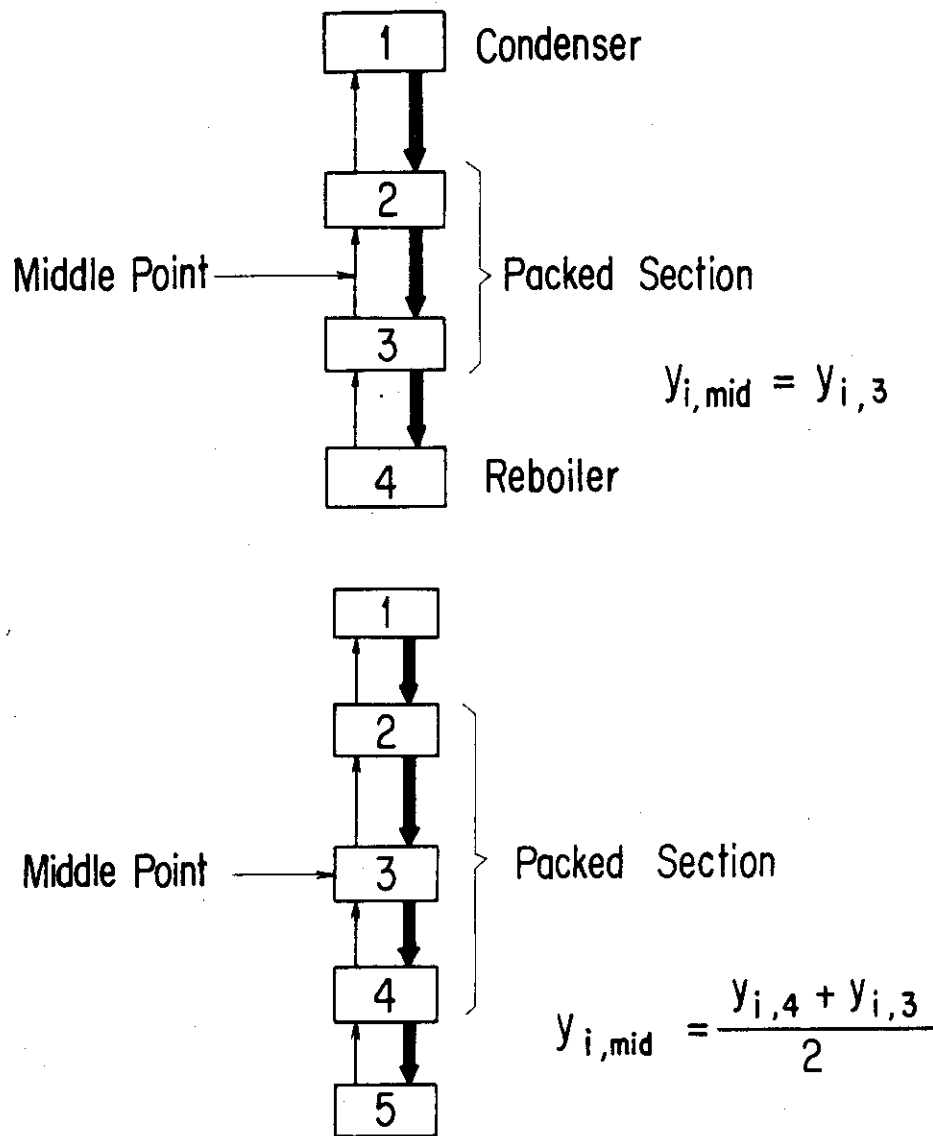


Fig. 8.2 Calculational procedure of argon concentration at the middle on a digital computer. The upper diagram is for cases where the number of total theoretical stages is even and the lower diagram is for cases where it is odd.

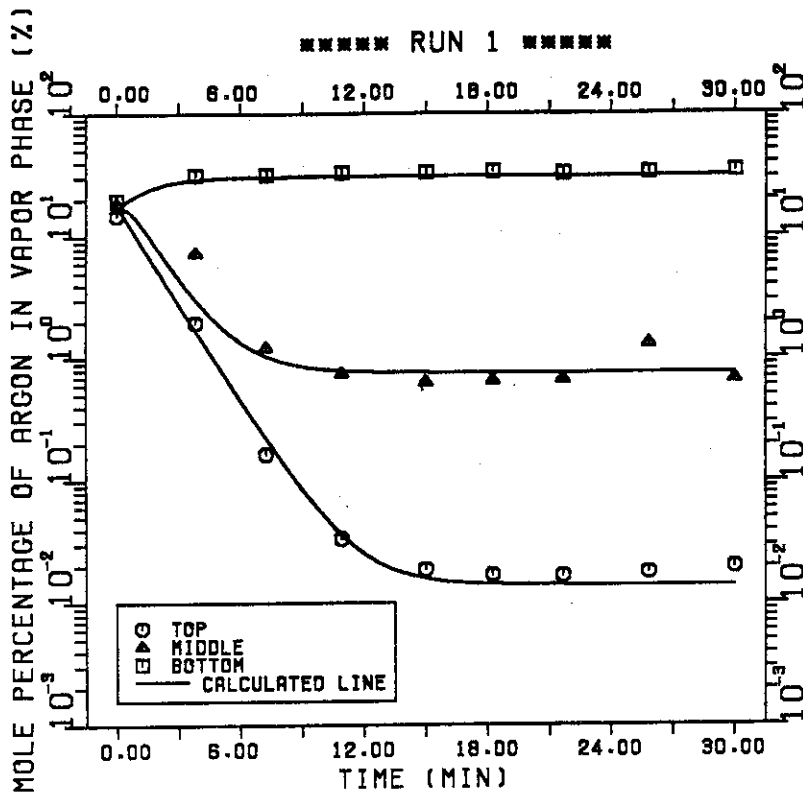


Fig. 8.3 An example of comparison between the calculation by a digital computer and the experimental observation.<sup>1)</sup> The vapor velocity is ~ 28 cm/sec. The number of total theoretical stages is 11. The packed section has 9 stages, so the HETP value is ~ 5.5 cm. Both the steady state and dynamic column behaviors are well described by the computer simulation.

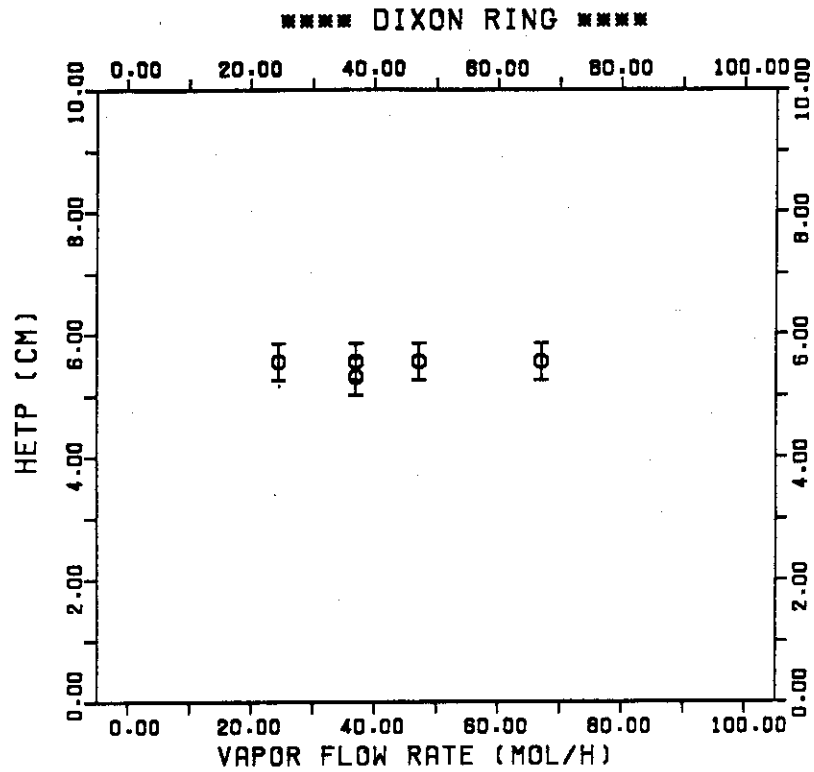


Fig. 8.4 Dependence of HETP on the vapor velocity within the column. The value of HETP is plotted against the vapor flow rate. The constancy of HETP is a feature of columns with small inner diameters ( $< 3$  cm).<sup>6)</sup>

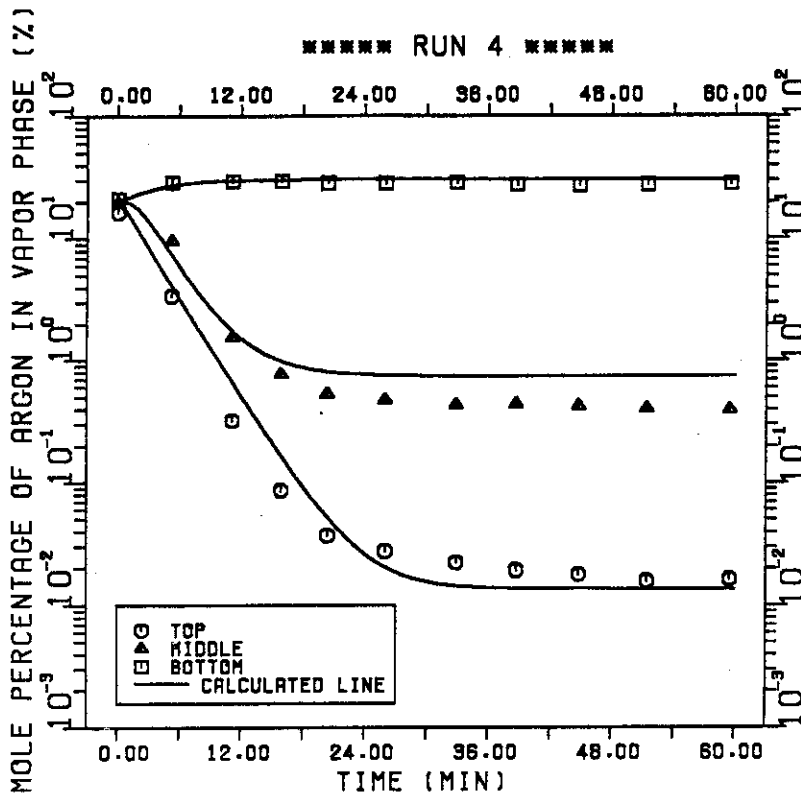


Fig. 8.5 An example of comparison between the calculation by a digital computer and the experimental observation. The vapor velocity is ~ 10 cm/sec. The number of total stages is 11.

## ACKNOWLEDGMENT

The author wishes to express his sincere thanks to Prof. Dr. T. Takamatsu (Kyoto Univ.), Dr. Y. Obata, Mr. Y. Naruse, Dr. K. Tanaka and Dr. H. Yoshida (JAERI) for their encouragement and guidance.

The studies described in chapters 4 and 7 were performed with Dr. J. R. Bartlit and Dr. R. H. Sherman (Los Alamos National Lab.). The study in chapter 8 was made possible by cooperation with Mr. T. Yamanishi (JAERI). Hence, these coworkers should greatly be thanked.

Valuable comments from Prof. Dr. T. Takamatsu, Dr. W. R. Wilkes (Mound Lab.) and Dr. P. C. Souers (Lawrence Livermore National Lab.) are truly appreciated.

Sincere appreciation should be expressed to Dr. J. L. Anderson (Los Alamos National Lab.) and Dr. J. E. Baublitz (U.S. Department of Energy) for promoting the US-Japan Fusion Cooperative Program.

The author,



Masahiro Kinoshita